



Quantum Rabi model with dissipation and qubit driving

L. O. Castanos-Cervantes ^{*}*Tecnologico de Monterrey, Escuela de Ingenieria y Ciencias, 14380 Ciudad de Mexico, CDMX, Mexico* (Received 2 January 2021; revised 4 August 2021; accepted 23 August 2021; published 13 September 2021)

We consider the quantum Rabi model as an open system that is subject to dissipation, dephasing, and sinusoidal qubit driving. One can change to an interaction picture where the qubit-driving term disappears at the expense of changing the free energy of the qubit which becomes time dependent. If the driving frequency is large with respect to the rest of the parameters with the exception of the driving strength, then one can obtain an effective Hamiltonian that accurately describes the dynamics of the system. The driving has two effects: the qubit-transition frequency is changed and the qubit has reduced dephasing. The driving strength can be chosen so that the qubit-transition frequency is reduced, made equal to zero, or even made negative so that the excited and ground states of the qubit are interchanged. Therefore, sinusoidal qubit driving offers another method to control the qubit-transition frequency and to reduce qubit dephasing. Adjusting the driving strength allows one to consider a qubit with degenerate energy levels. Not taking dissipation into account, the evolution operator of the qubit-harmonic oscillator system is given by a linear combination of the orthogonal projectors onto the eigenstates of $\hat{\sigma}_x$, followed by the evolution operator of a forced harmonic oscillator, the harmonic oscillator can be prepared in such a way that it is always found in a Schrödinger cat state, and the transition probability of the qubit can exhibit a collapse-revival behavior. In addition, the Born-Markov-secular master equation is deduced and the effects of dissipation are presented. In particular, smaller ultrastrong-coupling values are preferable over larger ultrastrong-coupling values and deep strong-coupling values in order to have long-lived, easily distinguishable Schrödinger cat states because the decoherence rate is inversely proportional to the square of the coupling. Finally, the qubit-harmonic oscillator system can be prepared in highly entangled states that are stable under dissipation.

DOI: [10.1103/PhysRevA.104.033709](https://doi.org/10.1103/PhysRevA.104.033709)

I. INTRODUCTION

The quantum Rabi model (QRM) is one of the fundamental models used to describe the interaction of light with matter [1]. It is also known as the *Jaynes-Cummings (JC) model without the rotating wave approximation (RWA)* [2,3], the *single-mode spin boson model* [4,5], and the *qubit-oscillator system* [6,7]. It can describe, for example, systems in cavity quantum electrodynamics (QED) consisting of atoms interacting with the electromagnetic field of a cavity [8,9], molecular dimers [2], and systems in circuit QED where artificial atoms (charge qubits or flux qubits) interact with the electromagnetic field of a transmission line or a superconducting quantum interference device [10,11].

The QRM consists of a two-level system (a qubit) interacting with a one-dimensional harmonic oscillator. It depends on three parameters: the transition frequency ω_s of the qubit, the frequency Ω of the harmonic oscillator, and the coupling strength $|g|$ between the qubit and the harmonic oscillator. Depending on the relationship between the three parameters and the energies to which the system can have access, the QRM can exhibit very different physics [11–13]. Assuming resonance $\omega_s = \Omega$, one can distinguish three regimes depending on which terms of the QRM Hamiltonian dominate the dy-

namics [12,14]: the perturbative ultrastrong-coupling (pUSC) regime, the nonperturbative ultrastrong-coupling and nonperturbative deep strong-coupling (npUSC and npDSC) regime, and the perturbative deep strong-coupling (pDSC) regime. The pUSC regime treats the interaction between the qubit and the harmonic oscillator as a perturbation and roughly spans the region $0.1 \lesssim |g/\Omega| \lesssim 0.3$. In this regime, the QRM can be accurately described by the Bloch-Siegert Hamiltonian [3,14]. The pDSC regime treats the interaction between the qubit and the harmonic oscillator as the dominant term and roughly spans the region $1 \lesssim |g/\Omega|$. In this regime, it can be accurately described by several approximate methods such as ordinary perturbation theory [14,15] and the *adiabatic approximation* [16]. Finally, the npUSC and npDSC regime does not treat any term as a perturbation and roughly considers $0.3 \lesssim |g/\Omega| \lesssim 1$. Broadly speaking, one can refer simply to the ultrastrong-coupling (USC) regime as the region where $0.1 \lesssim |g/\Omega| \lesssim 1$ and to the deep strong-coupling (DSC) regime as the region where $1 \lesssim |g/\Omega|$. One must be careful with the numerical values given to define all these regimes because they consider *small* values of the energies. In general, they depend on the energies to which the system can have access. For example, for resonant situations $\omega_s = \Omega$ and *larger* values of the energy, the npUSC and npDSC regime can start (end) for smaller (larger) values of the coupling strength [14]. In addition to the approximate treatments mentioned above, there are others that can describe the QRM more accurately [4–7,17–20]. It is

*luis.castanos@tec.mx, LOCCJ@yahoo.com

usually easier to work with these than to use the exact solution [21–24].

The QRM model has had extensive applications in quairesonant situations $|\omega_s - \Omega| \ll \Omega$ where the interaction is a perturbation $|g/\Omega| \ll 1$. These conditions correspond to the pUSC regime and the QRM can be further simplified using the RWA to obtain the JC model. For example, the JC model has been applied to the experiments in cavity QED where $|g/\Omega| \lesssim 10^{-6}$ [8,9,12]. On the other hand, there has been great progress in the area of solid-state systems where coupling strengths $|g/\Omega|$ corresponding to the npUSC [25,26] and the DSC [27,28] regimes have been obtained. Even some cold atom systems have reached the USC regime [29]. This has driven research of the QRM and its extensions in the USC and DSC regimes. In particular, important applications in quantum computing have been developed such as ultrafast two-qubit gates [30], frequency conversion [31], and quantum simulations [32,33]. In addition, very interesting and often counterintuitive physical phenomena have been found. For example, it has been shown that the ground state of the QRM contains virtual photons [34]. If the two-level system interacting with the harmonic oscillator in the USC regime is built from the excited states of a three-level system, then the aforementioned virtual photons can be spontaneously converted into measurable photons [35]. Also, it has been found that a single photon can reversibly excite simultaneously several independent qubits without splitting the initial photon [36] and that the system can be strongly protected against dissipation or dephasing [37,38]. For an extensive discussion on USC and DSC phenomena see [11–13].

In this paper we consider the QRM as an open system that is subject to dissipation, dephasing, and qubit driving. In particular, we are interested in situations where the RWA cannot be applied to the qubit driving. First, it is shown that one can change to an interaction picture (IP) where the qubit-driving term disappears at the expense of changing the free energy of the qubit which becomes time dependent. Second, if the qubit-driving frequency is large with respect to the rest of the parameters with the exception of the qubit-driving strength, then one can average the interaction picture von Neumann equation to obtain an effective Hamiltonian that accurately describes the dynamics of the system. In this effective Hamiltonian there are two effects of the driving: the qubit-transition frequency is changed and the qubit has reduced dephasing. One can choose the qubit-driving strength so that qubit-transition frequency is reduced, made equal to zero, or even made negative so that the excited and ground states of the qubit are interchanged. Hence, it is shown that qubit driving offers another method to control the qubit-transition frequency and to reduce qubit dephasing. Third, adjusting the qubit-driving strength allows one to consider a qubit with degenerate energy levels. In particular, not taking dissipation into account, it is shown that the harmonic oscillator can be prepared in such a way that it is always found in a Schrödinger cat state. This is particularly relevant to quantum information where these states have been used for quantum error correction [39]. Also, it is shown that the transition probability of the qubit can exhibit a collapse-revival behavior. Then, the Born-Markov-secular master equation is deduced and the effects of dissipation and dephasing are presented. Finally,

it is shown that the qubit-harmonic oscillator system can be prepared in highly entangled states that are stable under dissipation.

It is important to mention that there are many studies considering the effects of qubit driving on the qubit dynamics [40–46]. In particular, its effects on spontaneous emission (enhancement and inhibition) have been studied both in the RWA [41] and without the RWA (see [42] and references therein). Moreover, if the qubit driving (in the RWA) is frequency or phase modulated, then qubit population-trapping states exist [43] and there can be complete population inversion even without a resonant interaction [40]. In addition, slowing down of decoherence can be achieved through frequency modulation of the qubit-heat bath coupling [44].

The paper is organized as follows. In Sec. II we introduce the model. In Secs. III and IV we, respectively, present the aforementioned unitary transformation and effective Hamiltonian. In Sec. V we consider a qubit with degenerate energy levels and study the dynamics of the system. The conclusions are in Sec. VI.

II. THE MODEL

The complete system is composed of a driven qubit S , a harmonic oscillator F , and three thermal baths B_j ($j = 1, 2, 3$) responsible for introducing dissipation and dephasing to the open system $S + F$.

The ground state of the qubit is $|1\rangle$, while its excited state is $|2\rangle$. The qubit raising and lowering operators are, respectively, given by

$$\hat{\sigma}_+ = |2\rangle\langle 1|, \quad \hat{\sigma}_- = \hat{\sigma}_+^\dagger = |1\rangle\langle 2|, \quad (1)$$

while the Pauli operators are

$$\begin{aligned} \hat{\sigma}_x &= \hat{\sigma}_- + \hat{\sigma}_+, & \hat{\sigma}_z &= |2\rangle\langle 2| - |1\rangle\langle 1|, \\ \hat{\sigma}_y &= i(\hat{\sigma}_- - \hat{\sigma}_+), & \hat{\sigma} &= \hat{\mathbf{x}}\hat{\sigma}_x + \hat{\mathbf{y}}\hat{\sigma}_y + \hat{\mathbf{z}}\hat{\sigma}_z. \end{aligned} \quad (2)$$

Here $\hat{\mathbf{x}}$, $\hat{\mathbf{y}}$, and $\hat{\mathbf{z}}$ are unit vectors along the positive directions of the x , y , and z axes. The qubit's state space \mathcal{H}_S has the orthonormal bases $\beta_{sz} = \{|2\rangle, |1\rangle\}$ and $\beta_{sx} = \{|+\rangle_x, |-\rangle_x\}$ with

$$|\pm\rangle_x = \frac{1}{\sqrt{2}}(|2\rangle \pm |1\rangle). \quad (3)$$

The former is composed of eigenvectors of $\hat{\sigma}_z$, while the latter is composed of eigenvectors of $\hat{\sigma}_x$:

$$\hat{\sigma}_z|2\rangle = |2\rangle, \quad \hat{\sigma}_z|1\rangle = -|1\rangle, \quad \hat{\sigma}_x|\pm\rangle_x = \pm|\pm\rangle_x. \quad (4)$$

The Hamiltonian of the driven qubit is

$$\hat{H}_{ds}(t) = \frac{\hbar\omega_s}{2}\hat{\sigma}_z - \hbar\Omega_d\cos(\omega_d t)\hat{\sigma}_x. \quad (5)$$

Here $\omega_s > 0$ is the qubit transition angular frequency, $\omega_d > 0$ is the driving angular frequency, and $\Omega_d > 0$ is the driving strength.

The harmonic oscillator F has angular frequency $\Omega > 0$ and its state space \mathcal{H}_F has the orthonormal basis $\beta_F = \{|n\rangle : n = 0, 1, 2, \dots\}$ where $|n\rangle$ is a number state. Also, \hat{a}^\dagger and \hat{a} are the creation and annihilation operators of the harmonic oscillator, respectively, so $[\hat{a}, \hat{a}^\dagger] = 1$ and

$$\hat{a}^\dagger|n\rangle = \sqrt{n+1}|n+1\rangle, \quad \hat{a}|n\rangle = \sqrt{n}|n-1\rangle. \quad (6)$$

The free Hamiltonian of the harmonic oscillator is

$$\hat{H}_F = \hbar\Omega\hat{a}^\dagger\hat{a}. \quad (7)$$

B_j ($j = 1, 2, 3$) is a thermal bath of harmonic oscillators. Its state space is \mathcal{H}_{B_j} and \hat{a}_{jk}^\dagger and \hat{a}_{jk} are the respective creation and annihilation operators of the k th oscillator of B_j . The thermal baths are independent, so the following commutation relations are satisfied:

$$[\hat{a}_{jk}, \hat{a}_{j'k'}] = [\hat{a}_{jk}^\dagger, \hat{a}_{j'k'}^\dagger] = 0, \quad [\hat{a}_{jk}, \hat{a}_{j'k'}^\dagger] = \delta_{jj'}\delta_{kk'}, \quad (8)$$

with δ_{jk} the Kronecker delta. The free Hamiltonian of B_j is

$$\hat{H}_{B_j} = \sum_k \hbar\omega_{jk}\hat{a}_{jk}^\dagger\hat{a}_{jk}, \quad (9)$$

with $\omega_{jk} > 0$ the angular frequency of the k th oscillator of B_j . The thermal baths B_1 and B_2 introduce dissipation and dephasing to S and F , respectively, while B_3 models additional dephasing processes of S .

The complete system $S + F + \sum_{j=1}^3 B_j$ has the state space $\mathcal{H} = \mathcal{H}_S \otimes \mathcal{H}_F \otimes_{j=1}^3 \mathcal{H}_{B_j}$ and density operator $\hat{\rho}(t)$. Its Hamiltonian is

$$\hat{H}(t) = \hat{H}_{ds}(t) + \hat{H}_F + \sum_{j=1}^3 \hat{H}_{B_j} - \sum_{j=0}^3 \hbar\hat{A}_j\hat{E}_j, \quad (10)$$

where $-\hbar\hat{A}_j\hat{E}_j$ are the interactions between the different subsystems. The operators are given by

$$\hat{A}_j = \begin{cases} \hat{\sigma}_x & \text{if } j = 0, 1, \\ \hat{a}^\dagger + \hat{a} & \text{if } j = 2, \\ |2\rangle\langle 2| & \text{if } j = 3 \end{cases} \quad (11)$$

and

$$\hat{E}_j = \begin{cases} g\hat{a}^\dagger + g^*\hat{a} & \text{if } j = 0, \\ \sum_k (g_{1k}\hat{a}_{1k}^\dagger + g_{1k}^*\hat{a}_{1k}) & \text{if } j = 1, \\ \sum_k (\kappa_k\hat{a}_{2k}^\dagger + \kappa_k^*\hat{a}_{2k}) & \text{if } j = 2, \\ \sum_{k,l} g_{3kl}\hat{a}_{3k}^\dagger\hat{a}_{3l} & \text{if } j = 3. \end{cases} \quad (12)$$

Here and in the following z^* denotes the complex conjugate of the complex number z . Also, g , g_{1k} , and κ_k are complex numbers with units of $1/s$, while g_{3kl} are real numbers with units $1/s$ that satisfy

$$g_{3kl} = g_{3lk}, \quad (13)$$

so that \hat{E}_3 is a hermitian operator. Notice that all the \hat{A}_j and \hat{E}_j are hermitian operators. The parameters $|g|$, $|g_{1k}|$, $|g_{3kl}|$, and $|\kappa_k|$ represent the *coupling strengths* between the various subsystems.

In all that follows assume that the initial density operator $\hat{\rho}(0)$ can be factored as

$$\hat{\rho}(0) = \hat{\rho}_{SF}(0) \otimes \hat{\rho}_{B_1}(0) \otimes \hat{\rho}_{B_2}(0) \otimes \hat{\rho}_{B_3}(0), \quad (14)$$

where $\hat{\rho}_{SF}(0)$ and $\hat{\rho}_{B_j}(0)$ are the initial density operators of $S + F$ and B_j , respectively. We assume that $\hat{\rho}_{B_j}(0)$ is a thermal

state at temperature $T > 0$:

$$\hat{\rho}_{B_j}(0) = \prod_k \hat{\rho}_{jk}(0), \quad \hat{\rho}_{jk}(0) = \frac{1}{Z_{jk}} e^{-\beta_{jk}\hat{a}_{jk}^\dagger\hat{a}_{jk}}, \quad (15)$$

with k_B the Boltzmann constant and

$$\beta_{jk} = \frac{\hbar\omega_{jk}}{k_B T}, \quad Z_{jk} = N(\omega_{jk}, T) + 1, \quad (16)$$

$$N(\omega, T) = \frac{1}{e^{\hbar\omega/(k_B T)} - 1}.$$

Note that $\hat{\rho}_{jk}(0)$ is the density operator at time $t = 0$ of the k th oscillator of B_j and that it is a thermal state. Also, the expected value at time $t = 0$ of the number operator $\hat{a}_{jk}^\dagger\hat{a}_{jk}$ of the k th oscillator of B_j satisfies

$$\langle \hat{a}_{jk}^\dagger\hat{a}_{jk} \rangle(0) = \text{Tr}_{jk}[\hat{\rho}_{jk}(0)\hat{a}_{jk}^\dagger\hat{a}_{jk}] = N(\omega_{jk}, T). \quad (17)$$

Here Tr_{jk} denotes the trace with respect to the degrees of freedom of the k th oscillator of B_j .

We are interested in determining the Born-Markov-secular master equation governing the evolution of the density operator of $S + F$. In order to do this, it is convenient to rewrite the Hamiltonian $\hat{H}(t)$ so that the interactions between $S + F$ and the thermal baths have an expected value equal to zero at time $t = 0$. One gets

$$\hat{H}(t) = \hat{H}_0(t) - \frac{\hbar}{2}\delta_3, \quad (18)$$

where

$$\hat{H}_0(t) = \frac{\hbar(\omega_s - \delta_3)}{2}\hat{\sigma}_z - \hbar\Omega_d \cos(\omega_d t)\hat{\sigma}_x + \hat{H}_F + \sum_{j=1}^3 \hat{H}_{B_j} - \sum_{j=0}^2 \hbar\hat{A}_j\hat{E}_j - \hbar\hat{A}_3(\hat{E}_3 - \delta_3), \quad (19)$$

and

$$\delta_3 = \text{Tr}_{B_3}[\hat{E}_3\hat{\rho}_{B_3}(0)] = \sum_k g_{3kk}N(\omega_{3k}, T). \quad (20)$$

Here, $\text{Tr}_{B_3}[\cdot]$ is the trace over the degrees of freedom of B_3 . Notice that the transition frequency ω_s of the qubit is shifted by $-\delta_3$ and that δ_3 is subtracted from the operator \hat{E}_3 in (19). In general, $|\delta_3| < \omega_s$ is a small frequency shift.

It follows that von Neumann's equation governing the evolution of $\hat{\rho}(t)$ takes the form

$$i\hbar\frac{d}{dt}\hat{\rho}(t) = [\hat{H}_0(t), \hat{\rho}(t)]. \quad (21)$$

In the next section we are going to apply a unitary transformation that is going to eliminate the qubit-driving term at the expense of changing $\hat{\sigma}_z$ by a projection of $\hat{\sigma}$ in the yz -plane. This will later allow us to obtain an effective Hamiltonian where an effect of the driving consists in changing the transition frequency of the qubit.

III. THE UNITARY TRANSFORMATION

We now pass to an IP defined by the unitary transformation

$$\begin{aligned} \hat{U}_{IS}(t) &= e^{-ib_0 t_2} [e^{\frac{1}{2}\theta(t_1)}|+\rangle_{xx}\langle +| + e^{-\frac{1}{2}\theta(t_1)}|-\rangle_{xx}\langle -|] \\ &= e^{-ib_0 t_2} e^{\frac{1}{2}\theta(t_1)\hat{\sigma}_x}, \end{aligned} \quad (22)$$

where

$$\begin{aligned} t_1 &= \omega_d t, & \theta(t_1) &= 2 \left(\frac{\Omega_d}{\omega_d} \right) \sin(t_1), \\ t_2 &= (\omega_s - \delta_3)t, & b_0 &= \frac{1}{2} \left[1 - J_0 \left(2 \frac{\Omega_d}{\omega_d} \right) \right], \end{aligned} \quad (23)$$

and J_0 is the Bessel function of the first kind of order zero [47]. Note that $\hat{U}_{IS}(t)$ is an operator of S .

Observe that $\hat{U}_{IS}(t)$ is designed to eliminate the qubit-driving term, since

$$\frac{d}{dt} \hat{U}_{IS}(t) = i[-b_0(\omega_s - \delta_3) + \Omega_d \cos(\omega_d t) \hat{\sigma}_x] \hat{U}_{IS}(t). \quad (24)$$

For clarity, operators in the IP have a subindex I : if $\hat{A}(t)$ is a linear operator in the Schrödinger picture (SP), then $\hat{A}_I(t)$ is the corresponding operator in the IP with

$$\hat{A}_I(t) = \hat{U}_{IS}^\dagger(t) \hat{A}(t) \hat{U}_{IS}(t). \quad (25)$$

The evolution equation for $\hat{\rho}_I(t)$ takes the form

$$\frac{d}{dt} \hat{\rho}_I(t) = -\frac{i}{\hbar} [\hat{H}_I(t_1), \hat{\rho}_I(t)], \quad (26)$$

with

$$\begin{aligned} \hat{H}_I(t_1) &= \frac{\hbar(\omega_s - \delta_3)}{2} \hat{\sigma} \cdot \hat{\mathbf{u}}(t_1) + \hat{H}_F - \sum_{j=0}^2 \hbar \hat{A}_j \hat{E}_j + \sum_{j=1}^3 \hat{H}_{B_j} \\ &\quad - \frac{\hbar}{2} [\hat{I}_s + \hat{\sigma} \cdot \hat{\mathbf{u}}(t_1)] (\hat{E}_3 - \delta_3), \end{aligned} \quad (27)$$

\hat{I}_s the identity operator of S , and

$$\hat{\mathbf{u}}(t_1) = -\sin[\theta(t_1)] \hat{\mathbf{y}} + \cos[\theta(t_1)] \hat{\mathbf{z}}. \quad (28)$$

Comparing (26) and (27) with (19) and (21) and using $|2\rangle\langle 2| = (1/2)(\hat{I}_s + \hat{\sigma}_z)$, one finds that the effect of the unitary transformation is to eliminate the driving term $-\hbar\Omega_d \cos(\omega_d t) \hat{\sigma}_x$ and to replace $\hat{\sigma}_z$ by $\hat{\sigma} \cdot \hat{\mathbf{u}}(t_1)$.

Notice that $\hat{\mathbf{u}}(t_1)$ is a unit vector in the yz plane that performs a *symmetric rotation* around $\hat{\mathbf{x}}$: it rotates back and forth around $\hat{\mathbf{x}}$ so that it forms a maximum angle $2\Omega_d/\omega_d$ and a minimum angle $-2\Omega_d/\omega_d$ with the positive z axis. In particular, it starts out as $\hat{\mathbf{z}}$ at time $t = 0$, rotates counterclockwise around $\hat{\mathbf{x}}$ until it forms a maximum angle $2\Omega_d/\omega_d$ with the positive z axis, and then rotates clockwise around $\hat{\mathbf{x}}$ until it forms a minimum angle $-2\Omega_d/\omega_d$ with the positive z axis. Afterwards, it again rotates counterclockwise around $\hat{\mathbf{x}}$ until it forms a maximum angle $2\Omega_d/\omega_d$ with the positive z axis and the process repeats itself. In particular, $\hat{\mathbf{u}}(t_1)$ is t periodic with period $2\pi/\omega_d$.

The behavior of $\hat{\mathbf{u}}(t_1)$ described in the preceding paragraph provides the geometric picture needed to intuitively understand the *averaging* or *rotating wave approximation* to be performed in the next section. Assume ω_d is much larger than the rest of the frequencies and coupling strengths appearing in $\hat{H}_I(t_1)$ with the exception of Ω_d (Ω_d only affects the maximum and minimum angles mentioned in the preceding paragraph). Since each term of $\hat{H}_I(t_1)$ is multiplied by a frequency or coupling strength much smaller than ω_d , it follows that $\hat{\rho}_I(t)$ is going to remain approximately constant in a time interval of length $2\pi/\omega_d$ while $\hat{\mathbf{u}}(t_1)$ performs a complete *symmetric*

rotation. Then, $\hat{\rho}_I(t)$ only sees the average of $\hat{\mathbf{u}}(t_1)$ in this time interval and one can average von Neumann's equation (26) in a t interval of length $2\pi/\omega_d$ to obtain an approximate equation describing accurately the evolution of $\hat{\rho}_I(t)$. This *averaging* is usually called the *rotating wave approximation* and it is based on the *averaging theorem* of dynamical systems [48].

To end this section we comment more on $\hat{U}_{IS}(t)$. References [45,46] considered a sinusoidally driven qubit with large detuning $\omega_s \ll \omega_d$ or $\omega_d \ll \omega_s$ (say, $\omega_s \leq 0.1\omega_d$ or $\omega_d \leq 0.1\omega_s$) and presented very simple, analytic, and accurate formulas describing the evolution of the Bloch vector of the qubit. From them one can deduce that an accurate approximation to the evolution operator of a sinusoidally driven qubit in the blue detuned regime $\omega_s \ll \omega_d$ is

$$\hat{U}_{IS}(t) e^{-\frac{i}{2} J_0(2\Omega_d/\omega_d) t_2 \hat{\sigma}_z}. \quad (29)$$

We emphasize that (29) is an accurate approximation to the evolution operator associated with the Hamiltonian $\hat{H}_{ds}(t)$ in (5) if one takes $\delta_3 = 0$ in $\hat{U}_{IS}(t)$ and one considers $\omega_s \ll \omega_d$. It was obtained by the method of multiple scales [45]. The second factor in (29) was not used here for the IP so that $(\hat{\sigma}_x)_I(t) = \hat{\sigma}_x$.

IV. THE AVERAGED EQUATION

In the rest of the paper assume that the frequencies and coupling strengths satisfy

$$\begin{aligned} \left| \frac{\omega_s}{\omega_d}, \frac{\Omega}{\omega_d}, \frac{\omega_{jk}}{\omega_d}, \frac{\delta_3}{\omega_d} \right| &\ll 1, \\ \left| \frac{g}{\omega_d}, \frac{g_{1k}}{\omega_d}, \frac{g_{3kl}}{\omega_d}, \frac{\kappa_k}{\omega_d} \right| &\ll 1. \end{aligned} \quad (30)$$

Since (30) is satisfied and $\hat{H}_I(t_1) = \hat{H}_I(\omega_d t)$ is t periodic with period $2\pi/\omega_d$, one can average von Neumann's IP equation (26) in a t interval of length $2\pi/\omega_d$ (see Appendix A for the details). One obtains the averaged equation

$$\frac{d}{dt} \hat{\rho}_I^{\text{avg}}(t) = -\frac{i}{\hbar} [\hat{H}_I^{\text{avg}}, \hat{\rho}_I^{\text{avg}}(t)], \quad (31)$$

with the averaged Hamiltonian

$$\begin{aligned} \hat{H}_I^{\text{avg}} &= \frac{\hbar\omega_{so}}{2} \hat{\sigma}_z + \hat{H}_F + \sum_{j=1}^3 \hat{H}_{B_j} - \sum_{j=0}^2 \hbar \hat{A}_j \hat{E}_j \\ &\quad - \frac{\hbar}{2} \left[\hat{I}_s + J_0 \left(2 \frac{\Omega_d}{\omega_d} \right) \hat{\sigma}_z \right] (\hat{E}_3 - \delta_3), \end{aligned} \quad (32)$$

and the effective qubit frequency

$$\omega_{so} = (\omega_s - \delta_3) J_0 \left(2 \frac{\Omega_d}{\omega_d} \right). \quad (33)$$

Note that we have added the superscript *avg* to indicate that it is the averaged equation. One transforms back to the SP using the unitary transformation $\hat{U}_{IS}(t)$ in (22).

Comparing $\hat{H}_I(t_1)$ in (27) with \hat{H}_I^{avg} , one observes that \hat{H}_I^{avg} is obtained from $\hat{H}_I(t_1)$ by replacing $\hat{\sigma} \cdot \hat{\mathbf{u}}(t_1)$ by $J_0(2\Omega_d/\omega_d) \hat{\sigma}_z$, its average in a t_1 interval of length 2π .

Choosing the driving frequency ω_d so that (30) is satisfied leads to the effective IP Hamiltonian \hat{H}_I^{avg} in (32). Note that it has the same form of the QRM with dissipation and

that the qubit has the effective transition frequency ω_{so} in (33). Since $-0.403 \leq J_0(2\Omega_d/\omega_d) \leq 1$, one can adjust the driving parameters Ω_d/ω_d to control ω_{so} : it can take any value between $-0.403(\omega_s - \delta_3)$ and $(\omega_s - \delta_3)$. In particular, if $\Omega_d/\omega_d = 1.2025$, then $J_0(2\Omega_d/\omega_d) = 0$ and $\omega_{so} = 0$, so one obtains a qubit with degenerate energy levels and reduced dephasing because the qubit and the thermal bath B_3 are not coupled.

In the next sections we consider the case where Ω_d/ω_d is adjusted so that the qubit has degenerate energy levels.

V. DEGENERATE QUBIT LEVELS

If the driving strength and frequency are adjusted so that $\Omega_d/\omega_d = 1.2025$, then $J_0(2\Omega_d/\omega_d) = 0$ and the Hamiltonian (32) reduces to

$$\hat{H}_I^{\text{avg}} = \hat{H}_{\text{DL}} + \sum_{j=1}^3 \hat{H}_{B_j} - \sum_{j=1,2} \hbar \hat{A}_j \hat{E}_j - \frac{\hbar}{2} (\hat{E}_3 - \delta_3), \quad (34)$$

where

$$\hat{H}_{\text{DL}} = \hbar \Omega \hat{a}^\dagger \hat{a} - \hbar \hat{\sigma}_x (g \hat{a}^\dagger + g^* \hat{a}). \quad (35)$$

Notice that \hat{H}_{DL} is the Hamiltonian of the quantum Rabi model where the qubit has degenerate energy levels. Also, observe from (34) that the qubit is subject to reduced dephasing because it is no longer coupled to B_3 .

The unitary transformation $\hat{U}_{IS}(t)$ in (22) can be used to return to the SP. Using $\hat{\rho}(t) = \hat{U}_{IS}(t) \hat{\rho}_I^{\text{avg}}(t) \hat{U}_{IS}^\dagger(t)$ and that $\hat{U}_{IS}(t)$ commutes with \hat{H}_I^{avg} in (34), it follows from (31) that the evolution equation for the density operator $\hat{\rho}(t)$ in the SP is

$$\frac{d}{dt} \hat{\rho}(t) = -\frac{i}{\hbar} [\hat{H}_I^{\text{avg}} - \hbar \Omega_d \cos(\omega_d t) \hat{\sigma}_x, \hat{\rho}(t)], \quad (36)$$

with \hat{H}_I^{avg} in (34). In the rest of the paper we use (36).

Note from (36) that, in the SP, the qubit still has degenerate energy levels and is still uncoupled to the thermal bath B_3 . Moreover, observe that the difference between the SP and IP Hamiltonians is the driving $-\hbar \Omega_d \cos(\omega_d t) \hat{\sigma}_x$. One eliminates the driving by using $\hat{U}_{IS}(t)$ in (22).

We are interested in determining the master equation governing the evolution of the density operator of $S + F$. In addition, we want to identify the effects of dissipation. In order to do this one requires the spectrum of \hat{H}_{DL} and its associated evolution operator. This is presented in the next sections.

A. Eigenvectors and eigenvalues of \hat{H}_{DL}

To determine the eigenvalues and eigenvectors of \hat{H}_{DL} , it is convenient to use coherent states and the displacement operator of the harmonic oscillator [49]. Coherent states are denoted by $|\gamma\rangle$ with γ a complex number and the displacement operator is the unitary operator

$$\hat{D}(\gamma) = e^{\gamma \hat{a}^\dagger - \gamma^* \hat{a}}. \quad (37)$$

Some very useful properties of the displacement operator that are used frequently are given in Appendix B.

The first step is to express both \hat{I}_x and $\hat{\sigma}_x$ in terms of projectors onto the eigenvectors $|\pm\rangle_x$ of $\hat{\sigma}_x$ so that

$$\hat{H}_{\text{DL}} = \hat{H}_1 |+\rangle_{xx} \langle +| + \hat{H}_2 |-\rangle_{xx} \langle -|, \quad (38)$$

where

$$\begin{aligned} \hat{H}_j &= \hbar \Omega \hat{a}^\dagger \hat{a} + (-1)^j \hbar (g \hat{a}^\dagger + g^* \hat{a}), \\ &= \hat{D}^\dagger \left[(-1)^j \frac{g}{\Omega} \right] \left[\hbar \Omega \hat{a}^\dagger \hat{a} - \hbar \frac{|g|^2}{\Omega} \right] \hat{D} \left[(-1)^j \frac{g}{\Omega} \right]. \end{aligned} \quad (39)$$

Making use of the eigenvectors of $\hat{\sigma}_x$ in (3), the number states $|n\rangle$, and the properties of the displacement operator in (B1), it follows from (38) and (39) that an orthonormal basis for the state space of $S + F$ composed of eigenvectors of \hat{H}_{DL} is

$$\begin{aligned} \beta &= \left\{ |\omega_n, -\rangle \equiv |-\rangle_x \otimes \hat{D}\left(-\frac{g}{\Omega}\right) |n\rangle, \right. \\ &\quad \left. |\omega_n, +\rangle \equiv |+\rangle_x \otimes \hat{D}\left(\frac{g}{\Omega}\right) |n\rangle : n = 0, 1, 2, \dots \right\}, \end{aligned} \quad (40)$$

with

$$\hat{H}_{\text{DL}} |\omega_n, \pm\rangle = \hbar \omega_n |\omega_n, \pm\rangle. \quad (41)$$

The eigenvalues of \hat{H}_{DL} are given by

$$\hbar \omega_n = \hbar \Omega \left(n - \frac{|g|^2}{\Omega^2} \right), \quad n = 0, 1, 2, \dots \quad (42)$$

Notice that they are all two-degenerate and that the spectrum of \hat{H}_{DL} is simply that of the harmonic oscillator translated by $-\hbar |g|^2/\Omega$.

B. Evolution operator associated with \hat{H}_{DL}

Using the orthonormal basis β in (40) it follows that the evolution operator associated with \hat{H}_{DL} is

$$\begin{aligned} e^{-\frac{i}{\hbar} \hat{H}_{\text{DL}} t} &= \sum_{n=0}^{+\infty} e^{-i\omega_n t} (|\omega_n, +\rangle \langle \omega_n, +| + |\omega_n, -\rangle \langle \omega_n, -|) \\ &= e^{\frac{i}{\hbar} \Phi(t)} \{ e^{-i\Omega \hat{a}^\dagger \hat{a} t} \hat{D}[-\alpha(t)] |+\rangle_{xx} \langle +| \\ &\quad + e^{-i\Omega \hat{a}^\dagger \hat{a} t} \hat{D}[\alpha(t)] |-\rangle_{xx} \langle -| \}, \end{aligned} \quad (43)$$

where

$$\Phi(t) = \hbar \frac{|g|^2}{\Omega^2} [\Omega t - \sin(\Omega t)], \quad \alpha(t) = \frac{g}{\Omega} (1 - e^{i\Omega t}). \quad (44)$$

For g real and not taking into account a global phase, $e^{-i\Omega \hat{a}^\dagger \hat{a} t} \hat{D}[\pm\alpha(t)]$ is the evolution operator of a forced harmonic oscillator with angular frequency Ω and forcing $-\hbar g \cos(\phi)(\hat{a}^\dagger + \hat{a})$ with $\phi = \pi$ for $+\alpha(t)$ and $\phi = 0$ for $-\alpha(t)$ [50]. Hence, the evolution operator is given by a linear combination of the orthogonal projectors onto the eigenstates $|\pm\rangle_x$ of $\hat{\sigma}_x$ followed by the evolution operator of a forced harmonic oscillator. Also, since the arguments $\pm\alpha(t)$ of the displacement operators in (43) differ by a minus sign, it follows that the evolution operator (43) can naturally lead to the formation of Schrödinger cat states in the harmonic oscillator.

If there are no thermal baths, the Hamiltonian of $S + F$ in the IP is given by \hat{H}_{DL} [see (34)], while the Hamiltonian of $S + F$ in the SP is given by $\hat{H}_{\text{DL}} - \hbar \Omega_d \cos(\omega_d t) \hat{\sigma}_x$ [see (36)]. Then, (43) is the evolution operator of $S + F$ in the IP if there

are no thermal baths. To determine the evolution operator of $S + F$ in the SP if there are no thermal baths, one can use the unitary transformation $\hat{U}_{IS}(t)$ in (22) and that $J_0(2\Omega_d/\omega_d) = 0$. One has

$$\hat{U}_{IS}(t)|\omega_n, \pm\rangle = e^{-\frac{i}{2}t_2} e^{\pm\frac{i}{2}\theta(t_1)} |\omega_n, \pm\rangle. \quad (45)$$

Using this result in (43), one obtains the evolution operator of $S + F$ in the SP if there are no thermal baths:

$$\begin{aligned} \hat{U}_{IS}(t)e^{-\frac{i}{\hbar}\hat{H}_{DL}t} &= e^{-\frac{i}{2}t_2} \sum_{n=0}^{+\infty} e^{-i\omega_n t} [e^{\frac{i}{2}\theta(t_1)} |\omega_n, +\rangle \langle \omega_n, +| \\ &\quad + e^{-\frac{i}{2}\theta(t_1)} |\omega_n, -\rangle \langle \omega_n, -|] \\ &= e^{\frac{i}{\hbar}\Phi(t)} e^{-\frac{i}{2}t_2} \{e^{\frac{i}{2}\theta(t_1)} e^{-i\Omega\hat{a}^\dagger\hat{a}t} \hat{D}[-\alpha(t)]|+\rangle_{xx}\langle +| \\ &\quad + e^{-\frac{i}{2}\theta(t_1)} e^{-i\Omega\hat{a}^\dagger\hat{a}t} \hat{D}[\alpha(t)]|-\rangle_{xx}\langle -|\}, \quad (46) \end{aligned}$$

with $\Phi(t)$ and $\alpha(t)$ given in (44). Observe that the relative phases $e^{\pm\frac{i}{2}\theta(t_1)/2}$ were added in addition to a global phase and that the eigenvectors of \hat{H}_{DL} are stationary states because they are only affected by a global phase. The evolution operator (46) is used in the next two sections to determine how the state of $S + F$ evolves without dissipation and dephasing.

1. Preparation of a Schrödinger cat state

In this section we show how to prepare $S + F$ in such a way that the harmonic oscillator is always found in a Schrödinger cat state. It only requires measuring the state of the qubit three times and the creation of the Schrödinger cat state is independent of the results of the measurements. We emphasize that we do not take into account the effects of dissipation and dephasing in this section. This is done in a later section. To determine the evolution of a state of $S + F$ we use (46), the evolution operator of $S + F$ in the SP if there are no thermal baths.

Assume that the state of $S + F$ is $|\omega_n, r\rangle$ with

$$r = \begin{cases} 1 & \text{if the initial state is } |\omega_n, +\rangle, \\ 2 & \text{if the initial state is } |\omega_n, -\rangle \end{cases} \quad (47)$$

for some $n = 0, 1, \dots$. Recall that this is an eigenstate of \hat{H}_{DL} and observe from (46) that this is a stationary state of the system.

The first step is to measure the state of the qubit to see if it is in the state $|1\rangle$ or $|2\rangle$. The state of $S + F$ immediately after the first measurement is

$$|\psi_1(0)\rangle = |j\rangle \otimes \hat{D}^\dagger \left[(-1)^r \frac{g}{\Omega} \right] |n\rangle, \quad (48)$$

where

$$j = \begin{cases} 1 & \text{if the first measurement result is } |1\rangle, \\ 2 & \text{if the first measurement result is } |2\rangle. \end{cases} \quad (49)$$

Now let the system evolve and measure the state of the qubit after a time $T_p = (2p - 1)\pi/\Omega$ with p a positive integer to see if it is in the state $|1\rangle$ or $|2\rangle$. The state of $S + F$ immediately after the second measurement is

$$|\psi_2(0)\rangle = |J\rangle \otimes \frac{1}{N_J} |K_J\rangle, \quad (50)$$

where

$$\begin{aligned} J &= \begin{cases} 1 & \text{if the second measurement result is } |1\rangle, \\ 2 & \text{if the second measurement result is } |2\rangle, \end{cases} \\ |K_J\rangle &= e^{i\theta(\omega_d T_p)/2} \hat{D} \left[2\frac{g}{\Omega} + (-1)^r \frac{g}{\Omega} \right] |n\rangle \\ &\quad + (-1)^{j+J} e^{-i\theta(\omega_d T_p)/2} \hat{D} \left[-2\frac{g}{\Omega} + (-1)^r \frac{g}{\Omega} \right] |n\rangle, \\ N_J &= \sqrt{\langle K_J | K_J \rangle}. \end{aligned} \quad (51)$$

Now let the system evolve and measure the state of the qubit after a time $T_q = (2q - 1)\pi/\Omega$ where q is a positive integer to see if it is in the state $|+\rangle_x$ or $|-\rangle_x$. The state of $S + F$ immediately after the third measurement is

$$|\psi_3(0)\rangle = |\pm\rangle_x \otimes \frac{1}{N_\pm} |\xi(0)\rangle, \quad (52)$$

with $N_\pm = \sqrt{\langle \xi(0) | \xi(0) \rangle}$ a normalization constant. Here

$$\begin{aligned} |\xi(0)\rangle &= e^{i\theta(\omega_d T_p)/2} \hat{D} \left[-(-1)^r \frac{g}{\Omega} \right] |n\rangle \\ &\quad + (-1)^{j+J} e^{-i\theta(\omega_d T_p)/2} \hat{D} \left[4\frac{g}{\Omega} - (-1)^r \frac{g}{\Omega} \right] |n\rangle, \end{aligned} \quad (53)$$

if the result of the third measurement was $|+\rangle_x$ and

$$\begin{aligned} |\xi(0)\rangle &= e^{i\theta(\omega_d T_p)/2} \hat{D} \left[-4\frac{g}{\Omega} - (-1)^r \frac{g}{\Omega} \right] |n\rangle \\ &\quad + (-1)^{j+J} e^{-i\theta(\omega_d T_p)/2} \hat{D} \left[-(-1)^r \frac{g}{\Omega} \right] |n\rangle, \end{aligned} \quad (54)$$

if the result of the third measurement was $|-\rangle_x$. Notice that $|\xi(0)\rangle$ is similar to a Schrödinger cat state.

Now simply let the system evolve. Using the evolution operator in (46) and omitting a global phase, the state of $S + F$ a time t after the third measurement is

$$|\psi_3(t)\rangle = |\pm\rangle_x \otimes \frac{1}{N_\pm} |\xi(t)\rangle. \quad (55)$$

To simplify the expression of $|\xi(t)\rangle$ define

$$\lambda_\pm(t) = \frac{1}{2}\theta(\omega_d T_p) \pm 2 \left| \frac{g}{\Omega} \right|^2 \sin(\Omega t). \quad (56)$$

First assume that the initial state of $S + F$ was $|\omega_n, +\rangle$. If the third measurement result was $|+\rangle_x$, then

$$\begin{aligned} |\xi(t)\rangle &= e^{i\lambda_-(t)} \hat{D} \left(\frac{g}{\Omega} \right) |n\rangle \\ &\quad + (-1)^{j+J} e^{-i\lambda_-(t)} \hat{D} \left[\frac{g}{\Omega} (1 + 4e^{-i\Omega t}) \right] |n\rangle. \end{aligned} \quad (57)$$

If the result of the third measurement was $|-\rangle_x$, then

$$\begin{aligned} |\xi(t)\rangle &= e^{i\lambda_+(t)} \hat{D} \left[-\frac{g}{\Omega} (1 + 2e^{-i\Omega t}) \right] |n\rangle \\ &\quad + (-1)^{j+J} e^{-i\lambda_+(t)} \hat{D} \left[-\frac{g}{\Omega} (1 - 2e^{-i\Omega t}) \right] |n\rangle. \end{aligned} \quad (58)$$

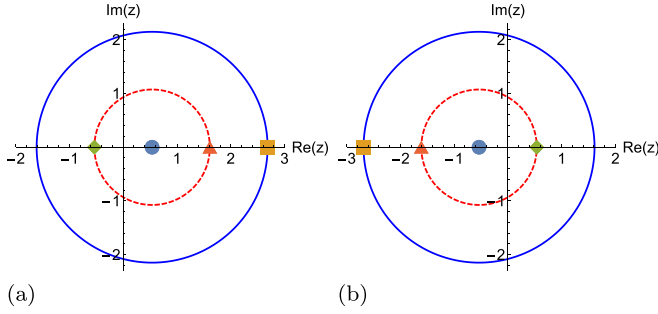


FIG. 1. Trajectories followed in the complex plane by the arguments z of the displacement operators appearing in the Schrödinger cat states (57)–(60) with $n = 0$. The cat states (57) and (60) have the form of a *solar system* with arguments $z = \pm g/\Omega$ (circle markers) and $\pm(g/\Omega)(1 + 4e^{-i\Omega t})$ (blue solid lines). The cat states (58) and (59) have the form of *end points of a rotating rigid bar* with arguments $z = \pm(g/\Omega)(1 + 2e^{-i\Omega t})$ and $\pm(g/\Omega)(1 - 2e^{-i\Omega t})$ (red dashed lines). The diamond, triangle, and square markers indicate the respective starting points: $z = \pm(g/\Omega)(1 - 2e^{-i\Omega t})$, $\pm(g/\Omega)(1 + 2e^{-i\Omega t})$, and $\pm(g/\Omega)(1 + 4e^{-i\Omega t})$ at $t = 0$. All trajectories rotate in the clockwise sense, $g/\Omega = 0.537$, and $\text{Re}(z)$ and $\text{Im}(z)$ are the real and imaginary parts of the dimensionless complex number z , respectively. The upper (lower) signs correspond to Figs. 1(a) and 1(b).

Now assume that the initial state of $S + F$ was $|\omega_n, -\rangle$. If the third measurement result was $|+\rangle_x$, then

$$|\xi(t)\rangle = e^{i\lambda_-(t)} \hat{D} \left[\frac{g}{\Omega} (1 - 2e^{-i\Omega t}) \right] |n\rangle + (-1)^{j+J} e^{-i\lambda_-(t)} \hat{D} \left[\frac{g}{\Omega} (1 + 2e^{-i\Omega t}) \right] |n\rangle. \quad (59)$$

If the result of the third measurement was $|-\rangle_x$, then

$$|\xi(t)\rangle = e^{i\lambda_+(t)} \hat{D} \left[-\frac{g}{\Omega} (1 + 4e^{-i\Omega t}) \right] |n\rangle + (-1)^{j+J} e^{-i\lambda_+(t)} \hat{D} \left(-\frac{g}{\Omega} \right) |n\rangle. \quad (60)$$

Observe from (57)–(60) that $|\xi(t)\rangle$ is a superposition of normalized, displaced number states the overlap of which is $e^{-16|g/\Omega|^2} [L_n(16|g/\Omega|^2)]^2$ with L_n the n th Laguerre polynomial. The overlap of two kets $|\psi_1\rangle$ and $|\psi_2\rangle$ is $|\langle\psi_1|\psi_2\rangle|^2$. For $n = 0$ and USC values $|g/\Omega| \geq 0.537$, the overlap is ≤ 0.01 and the harmonic oscillator is always in an easily distinguishable Schrödinger cat. In particular, if $n = 0$ (that is, the initial state of the system was $|\omega_0, \pm\rangle$), then $|\xi(t)\rangle$ is a Schrödinger cat state with the form of a *solar system* for (57) and (60) and with the form of *end points of a rotating rigid bar* for (58) and (59), as shown in Fig. 1. These types of states could be used in quantum information because they have been applied in quantum error correction [39].

2. Qubit and harmonic oscillator in their ground states

Assume that the initial state of $S + F$ is

$$|\psi(0)\rangle = |1\rangle \otimes |0\rangle, \quad (61)$$

that is, both the qubit and the harmonic oscillator are in their respective ground states. Using the evolution operator (46)

and omitting a global phase, the state of $S + F$ in the SP is

$$|\psi(t)\rangle = \frac{1}{2} [|2\rangle \otimes |\psi_-(t)\rangle + |1\rangle \otimes |\psi_+(t)\rangle], \quad (62)$$

where $|\psi_{\pm}(t)\rangle$ are superpositions of coherent states and have the form of Schrödinger cat states

$$|\psi_{\pm}(t)\rangle = e^{\frac{i}{2}\theta(t_1)} |-\alpha(t)e^{-i\Omega t}\rangle \pm e^{-\frac{i}{2}\theta(t_1)} |\alpha(t)e^{-i\Omega t}\rangle. \quad (63)$$

The overlap between the states comprising $|\psi_{\pm}(t)\rangle$ is

$$|\langle -\alpha(t)e^{-i\Omega t} | \alpha(t)e^{-i\Omega t} \rangle|^2 = \exp \left[-16 \left| \frac{g}{\Omega} \right|^2 \sin^2 \left(\frac{\Omega t}{2} \right) \right]. \quad (64)$$

This overlap takes on its maximum value 1 at times

$$T'_n = n \frac{2\pi}{\Omega}, \quad (n = 0, 1, 2, \dots). \quad (65)$$

Since $\alpha(T'_n) = 0$, the harmonic oscillator is in its ground state [see (44), (62), and (63)].

At any other times, $\alpha(t) \neq 0$ and $|\psi_{\pm}(t)\rangle$ are Schrödinger cat states. In particular, at times

$$T_n = (2n - 1) \frac{\pi}{\Omega}, \quad (n = 1, 2, \dots), \quad (66)$$

the overlap (64) takes on its minimum value

$$|\langle -\alpha(T_n)e^{-i\Omega T_n} | \alpha(T_n)e^{-i\Omega T_n} \rangle|^2 = \exp(-16|g/\Omega|^2), \quad (67)$$

and from (63) one has

$$|\psi_{\pm}(T_n)\rangle = e^{\frac{i}{2}\theta(\omega_d T_n)} \left| 2 \frac{g}{\Omega} \right\rangle \pm e^{-\frac{i}{2}\theta(\omega_d T_n)} \left| -2 \frac{g}{\Omega} \right\rangle. \quad (68)$$

Observe that (67) is $< 10^{-2}$ if $|g/\Omega| \geq 0.537$. Hence, one requires USC to have an easily distinguishable Schrödinger cat. If the interaction between the qubit and the harmonic oscillator is *tuned* to zero at a time T_n and one measures the state of the qubit at this time to see if it is in the state $|1\rangle$ or $|2\rangle$, then it follows from (62) that the harmonic oscillator would be in one of the states in (68) and, since it would evolve freely afterwards, it would remain in a Schrödinger cat state with the form of *end points of a rigid bar centered at the coordinate origin and rotating in the clockwise sense*:

$$e^{-\frac{i}{\hbar} \hat{H}_F(t-T_n)} |\psi_{\pm}(T_n)\rangle = e^{\frac{i}{2}\theta(\omega_d T_n)} \left| 2 \frac{g}{\Omega} e^{-i\Omega(t-T_n)} \right\rangle \pm e^{-\frac{i}{2}\theta(\omega_d T_n)} \left| -2 \frac{g}{\Omega} e^{-i\Omega(t-T_n)} \right\rangle. \quad (69)$$

To determine other properties, it is convenient to use the following operators:

$$\hat{X} = \frac{1}{\sqrt{2}} (\hat{a}^\dagger + \hat{a}), \quad \hat{P} = \frac{i}{\sqrt{2}} (\hat{a}^\dagger - \hat{a}). \quad (70)$$

Observe that $\sqrt{\hbar/(M\Omega)} \hat{X}$ and $\sqrt{M\hbar\Omega} \hat{P}$ would be the respective position and momentum operators of the harmonic oscillator if it has mass M [49] and that \hat{X} and \hat{P} are proportional to quadrature operators if the harmonic oscillator is a single mode of an electromagnetic field [51].

Given a linear operator $\hat{A}(t)$, we define the following expected values and root-mean-square (rms) deviations of $\hat{A}(t)$ in the states $|\pm \alpha(t)e^{-i\Omega t}\rangle$ comprising the Schrödinger cat

states in (63):

$$\begin{aligned}\langle \hat{A} \rangle_{\pm}^c(t) &= \langle \pm \alpha(t) e^{-i\Omega t} | \hat{A}(t) | \pm \alpha(t) e^{-i\Omega t} \rangle, \\ \Delta \hat{A}_{\pm}^c(t) &= \sqrt{\langle \hat{A}^2 \rangle_{\pm}^c(t) - \langle \hat{A} \rangle_{\pm}^c(t)^2}.\end{aligned}\quad (71)$$

Using the properties in (B1) it follows that

$$\begin{aligned}x_{\pm} &= \langle \hat{X} \rangle_{\pm}^c(t) = \mp \sqrt{2} \left| \frac{g}{\Omega} \right| [\cos(\delta) - \cos(\Omega t - \delta)], \\ p_{\pm} &= \langle \hat{P} \rangle_{\pm}^c(t) = \mp \sqrt{2} \left| \frac{g}{\Omega} \right| [\sin(\delta) + \sin(\Omega t - \delta)], \\ \Delta \hat{X}_{\pm}^c &= \Delta \hat{P}_{\pm}^c = \frac{1}{\sqrt{2}},\end{aligned}\quad (72)$$

$$\Delta(\hat{a}^{\dagger} \hat{a})_{\pm}^c(t) = \sqrt{\langle \hat{a}^{\dagger} \hat{a} \rangle_{\pm}^c(t)},$$

with

$$\begin{aligned}\frac{g}{\Omega} &= \left| \frac{g}{\Omega} \right| e^{i\delta}, \\ \langle \hat{a}^{\dagger} \hat{a} \rangle_{\pm}^c(t) &= \left[\frac{1}{\sqrt{2}} \langle \hat{X} \rangle_{\pm}^c(t) \right]^2 + \left[\frac{1}{\sqrt{2}} \langle \hat{P} \rangle_{\pm}^c(t) \right]^2.\end{aligned}\quad (73)$$

Since $|\pm \alpha(t) e^{-i\Omega t}\rangle$ are coherent states, we obtained $\Delta \hat{X}_{\pm}^c \Delta \hat{P}_{\pm}^c = 1/2$, that is, $|\pm \alpha(t) e^{-i\Omega t}\rangle$ are associated with minimum uncertainty wave packets. Also, observe that (x_{\pm}, p_{\pm}) are parametrizations of circumferences in the xp plane of radius $\sqrt{2}|g/\Omega|$ and centered at $\mp \sqrt{2}|g/\Omega|(\cos(\delta), \sin(\delta))$. Moreover, they trace out the circumferences in the clockwise sense with angular velocity Ω . Figure 2(a) illustrates the trajectories followed by (x_+, p_+) (red solid line) and (x_-, p_-) (blue dotted line) for $g/\Omega = 1$. Starting at the coordinate origin at $t = 0$, the arrows indicate the direction of the motion of $(x_+, p_+) = -(x_-, p_-)$. At times T'_n one has $(x_{\pm}, p_{\pm}) = (0, 0)$ and at times T_n the expected values $\langle \hat{X} \rangle_{\pm}^c(t)$ are the furthest away from each other. At these times T_n , the expected value $\langle \hat{a}^{\dagger} \hat{a} \rangle_{\pm}^c(t)$ is largest and the relative rms deviation $\Delta(\hat{a}^{\dagger} \hat{a})_{\pm}^c(t) / \langle \hat{a}^{\dagger} \hat{a} \rangle_{\pm}^c(t)$ is small because the former is one half of the square of the distance of (x_{\pm}, p_{\pm}) to the coordinate origin and the latter is $\sqrt{2}$ over the aforementioned distance. Recall that it is at one of these times T_n when one must measure the state of the qubit to see if it is in the state $|1\rangle$ or $|2\rangle$ and one must tune to zero the interaction between the qubit and the harmonic oscillator to obtain the most easily distinguishable Schrödinger cat state in (68) and (69).

From (62) it follows that the probability to find the qubit in the excited state $|2\rangle$ is

$$\begin{aligned}P_2(t) &= \frac{1}{2} \{1 - \text{Re}[e^{-i\theta(t_1)} \langle -\alpha(t) e^{-i\Omega t} | \alpha(t) e^{-i\Omega t} \rangle]\}, \\ &= \frac{1}{2} - \frac{1}{2} \cos[\theta(t_1)] \exp\left\{-4 \left| \frac{g}{\Omega} \right|^2 [1 - \cos(\Omega t)]\right\}\end{aligned}\quad (74)$$

with $\text{Re}(z)$ the real part of complex number z . $P_2(t)$ has the lower envelope

$$P_{2l}(t) = \frac{1}{2} - \frac{1}{2} \exp\left\{-4 \left| \frac{g}{\Omega} \right|^2 [1 - \cos(\Omega t)]\right\}, \quad (75)$$

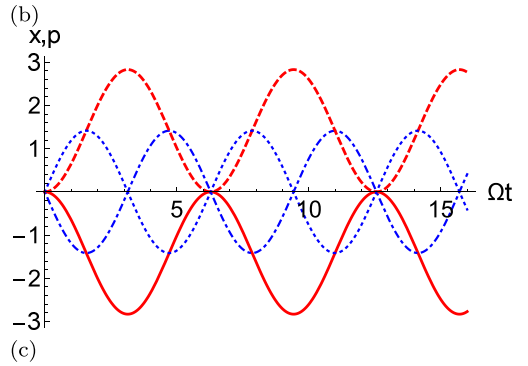
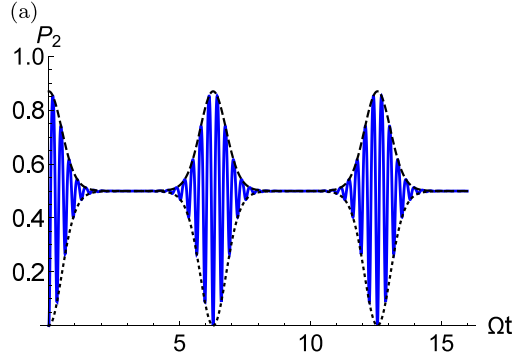
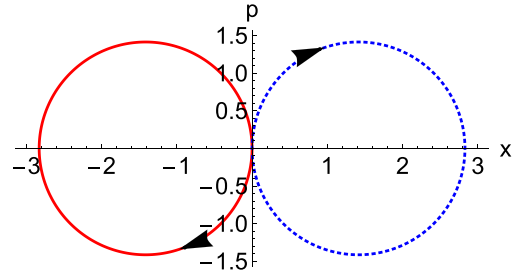


FIG. 2. (a) Parametric curves (x_+, p_+) (red solid line) and (x_-, p_-) (blue dotted line) defined in (72). The arrows indicate the direction of the motion. (b) Probability to find the qubit in the excited state $P_2(t)$ (blue solid line) and the envelopes $P_{2l}(t)$ (black dotted line) and $P_{2u}(t)$ (black dashed line) as functions of Ωt [see (74)–(76)]. (c) x_+ (red solid line), x_- (red dashed line), p_+ (blue dot-dashed line), and p_- (blue dotted line) as functions of Ωt . The values of the parameters are in (79).

and the upper envelope (with $\Omega_d/\omega_d = 1.2025$)

$$P_{2u}(t) = \frac{1}{2} - \frac{1}{2} \cos\left(2 \frac{\Omega_d}{\omega_d}\right) \exp\left\{-4 \left| \frac{g}{\Omega} \right|^2 [1 - \cos(\Omega t)]\right\}.\quad (76)$$

It gives an upper bound for the maximum value of $P_2(t)$:

$$P_{2\max} = \frac{1}{2} \left[1 - \cos\left(2 \frac{\Omega_d}{\omega_d}\right)\right] \simeq 0.87.\quad (77)$$

Notice that the envelopes are t -periodic functions with period $2\pi/\Omega$ and that the driving strength and frequency Ω_d/ω_d determine the maximum probability. In addition, observe that at times T_n in (66), $x_{\pm} = \langle \hat{X} \rangle_{\pm}^c(T_n)$ are furthest away from each

other and

$$P_{2u}(T_n) = \frac{1}{2} \left[1 - \cos \left(2 \frac{\Omega_d}{\omega_d} \right) e^{-8|g/\Omega|^2} \right],$$

$$P_{2l}(T_n) = \frac{1}{2} \left[1 - e^{-8|g/\Omega|^2} \right]. \quad (78)$$

These values reduce to $\simeq 0.5$ for large coupling strengths $|g/\Omega|$ (their distance to 0.5 is ≤ 0.01 if $|g/\Omega| \geq 0.76$), so it is approximately equal to find the qubit in the excited and ground states when $x_{\pm} = \langle \hat{X} \rangle_{\pm}^c(t)$ are furthest away from each other.

Figure 2(b) illustrates $P_2(t)$ (blue solid line) and the envelopes $P_{2l}(t)$ (black dotted line) and $P_{2u}(t)$ (black dashed line) for

$$\frac{\Omega_d}{\omega_d} = 1.2025, \quad \frac{g}{\Omega} = 1, \quad \frac{\Omega}{\omega_d} = 10^{-1}. \quad (79)$$

Observe that $P_2(t)$ oscillates between the envelopes in a form similar to a collapse revival, although the collapse is at $P_2 \simeq 0.5$. The oscillations are faster for smaller values of Ω/ω_d . Figure 2(c) illustrates x_{\pm} (red solid and red dashed lines) and p_{\pm} (blue dotted and blue dot-dashed lines) as functions of Ωt for the values in (79) [see the definitions in (72)]. Observe that in the neighborhood of the times T'_n when x_{\pm}, p_{\pm} are all close to zero, $P_2(t)$ exhibits large oscillations. Also, in the neighborhood of the times T_n when x_{\pm} are furthest away from zero, $P_2(t)$ collapses to a value $\simeq 0.5$. This behavior of $P_2(t)$ comes from the fact that it depends on the inner product between the states $|\pm \alpha(t)e^{-i\Omega t}\rangle$ [see the first line in (74)]. In the neighborhood of times T'_n the overlap is approximately 1 because x_{\pm}, p_{\pm} are all close zero. In the neighborhood of times T_n the overlap is approximately zero because x_{\pm} are furthest away from each other. It also follows that it is approximately equal to find the qubit in the ground and excited states when one measures at a time T_n its state to create the Schrödinger cat state in (68).

It is important to identify the effects of the driving in $P_2(t)$. The driving modifies the qubit transition frequency and introduces quantities depending on $\theta(t_1)$ [see (35), (43), and (46)]. If the qubit has degenerate energy levels and there is no driving [that is, it evolves according to (43)], then $\theta(t_1) = 0$ and the probability to find the qubit in the excited state $|2\rangle$ is $P_{2l}(t)$ in (75). Observe that $P_{2l}(t)$ has a maximum value < 0.5 and recall that it is illustrated in Fig. 2(b) as the lower black dotted line for the values in (79). Comparing $P_2(t)$ in (74) with $P_{2l}(t)$ in (75) one finds that the term $\cos[\theta(t_1)]$ comes from the driving, is responsible for the fast oscillations of $P_2(t)$ illustrated as a blue solid line in Fig. 2(b), and allows $P_2(t)$ to attain the much larger value $P_{2\max} \simeq 0.87$ in (77).

Finally, we comment on the accuracy of the results presented in this section. These are based on \hat{H}_{DL} in (35). Since this Hamiltonian is an approximation, it is important to determine the accuracy of the dynamics obtained from it.

First, recall that the exact Hamiltonian of the system in the IP is $\hat{H}_I(t_1)$ in (27). Then, we made assumption (30) and this allowed us to average the von Neumann IP equation (26) over a t interval of length $2\pi/\omega_d$ to obtain the averaged equation (31) with the averaged Hamiltonian \hat{H}_I^{avg} in (32) and the effective qubit frequency ω_{so} in (33). Finally, we assumed that the driving parameters satisfy $\Omega_d/\omega_d = 1.2025$, so $\omega_{so} = 0$

and \hat{H}_I^{avg} reduced to the form in (34). Hence, the dynamics obtained from \hat{H}_I^{avg} in (34) have to be compared with those of the exact Hamiltonian $\hat{H}_I(t_1)$ in (27) under assumptions (30) and $\Omega_d/\omega_d = 1.2025$. If there are no thermal baths, then \hat{H}_I^{avg} in (34) reduces to \hat{H}_{DL} in (35), $\hat{H}_I(t_1)$ in (27) takes the form

$$\hat{H}_I(t_1) = \frac{\hbar\omega_s}{2} \hat{\sigma} \cdot \hat{\mathbf{u}}(t_1) + \hbar\Omega \hat{a}^\dagger \hat{a} - \hbar\hat{\sigma}_x(g\hat{a}^\dagger + g^*\hat{a}), \quad (80)$$

and the assumptions reduce to

$$\frac{\omega_s}{\omega_d}, \frac{\Omega}{\omega_d}, \left| \frac{g}{\omega_d} \right| \ll 1, \quad \frac{\Omega_d}{\omega_d} = 1.2025. \quad (81)$$

Observe that the dynamics obtained from \hat{H}_{DL} are going to be more accurate for smaller values of the quantities on the left-hand side of (81) (see the argument given in Sec. III). To determine the accuracy quantitatively, we considered the initial condition in (61) and

$$\frac{\omega_s}{\Omega} = \frac{g}{\Omega} = 1, \quad \frac{\Omega}{\omega_d} = 10^{-2}, \quad \frac{\Omega_d}{\omega_d} = 1.2025. \quad (82)$$

Notice that these values correspond to conditions of resonance, USC, and the assumptions in (81). Then, we numerically solved the exact (nondimensional) Schrödinger equation

$$\frac{d}{d\tau} |\psi_{IN}(\tau)\rangle = -i \frac{\hat{H}_I(\tau)}{\hbar\omega_d} |\psi_{IN}(\tau)\rangle, \quad (83)$$

and calculated the overlap between the numerical solution $|\psi_{IN}(\tau)\rangle$ and the analytic solution $|\psi_I(\tau/\omega_d)\rangle = \hat{U}_{IS}^\dagger(\tau/\omega_d)|\psi(\tau/\omega_d)\rangle$ in the IP with $|\psi(\tau/\omega_d)\rangle$ in (62). We obtained $|\langle \psi_{IN}(\tau) | \psi_I(\tau/\omega_d) \rangle|^2 > 0.9998$ for the time interval $0 \leq \tau = \omega_d t \leq 10\pi(\omega_d/\Omega) = 3141.6$. Given these results, we conclude that the dynamics obtained from \hat{H}_{DL} accurately describe those obtained from $\hat{H}_I(t_1)$ for the values in (82) and the time interval $0 \leq \Omega t \leq 10\pi$.

C. Master equation

In this section we consider $S + F$ as an open quantum system interacting with the thermal baths. Applying a standard method [52] to the SP equation for $\hat{\rho}(t)$ in (36) with the averaged Hamiltonian in (34), one can calculate the Born-Markov-secular master equation in the Lindblad form governing the evolution of the $S + F$ density operator $\hat{\rho}_{\text{SF}}(t) = \text{Tr}_{B_1, B_2, B_3}[\hat{\rho}(t)]$ (here $\text{Tr}_{B_1, B_2, B_3}$ is the partial trace with respect to the thermal baths' degrees of freedom):

$$\frac{d}{dt} \hat{\rho}_{\text{SF}}(t) = -\frac{i}{\hbar} [\hbar\Omega' \hat{b}^\dagger \hat{b} - \hbar\Omega_d \cos(\omega_d t) \hat{\sigma}_x, \hat{\rho}_{\text{SF}}(t)] + \mathcal{D}[\hat{\rho}_{\text{SF}}(t)], \quad (84)$$

where the dissipator $\mathcal{D}(\cdot)$ is given by

$$\mathcal{D}(\hat{\rho}) = \gamma_0 N(\Omega, T) \left(\hat{b}^\dagger \hat{\rho} \hat{b} - \frac{1}{2} \{ \hat{b} \hat{b}^\dagger, \hat{\rho} \} \right) + \gamma_0 [N(\Omega, T) + 1] \left(\hat{b} \hat{\rho} \hat{b}^\dagger - \frac{1}{2} \{ \hat{b}^\dagger \hat{b}, \hat{\rho} \} \right) + \gamma_{00} \left(\hat{\sigma}_x \hat{\rho} \hat{\sigma}_x - \frac{1}{2} \{ \hat{\sigma}_x \hat{\sigma}_x, \hat{\rho} \} \right). \quad (85)$$

Here $N(\Omega, T)$ is defined in (16) and represents the mean number of B_2 thermal excitations (photons if B_2 is an electromagnetic field) at frequency Ω . Only Ω appears because the qubit has transition frequency $\omega_{so} = 0$ in all of Sec. V. Also, $\{\cdot, \cdot\}$ is the anticommutator and

$$\hat{b} = \hat{a} - \frac{g}{\Omega} \hat{\sigma}_x. \quad (86)$$

If $\rho_{Dj}(\omega)$ is the density of states where $\rho_{Dj}(\omega)d\omega$ gives the number of oscillators of B_j ($j = 1, 2$) with frequencies in the interval ω to $\omega + d\omega$, then the shifted frequency Ω' can be expressed using the principal value (PV) as

$$\Omega' = \Omega + \text{PV} \int_0^{+\infty} d\omega \rho_{D2}(\omega) |\kappa(\omega)|^2 \frac{2\omega}{\Omega^2 - \omega^2}, \quad (87)$$

the decay rate γ_0 is given by

$$\gamma_0 = 2\pi \rho_{D2}(\Omega) |\kappa(\Omega)|^2, \quad (88)$$

and the decay rate γ_{00} is defined by

$$\gamma_{00} = \gamma_1(0) + \gamma_{10}(0) + \left(\frac{g + g^*}{\Omega}\right)^2 [\gamma_2(0) + \gamma_{20}(0)], \quad (89)$$

with

$$\begin{aligned} \gamma_j(\omega') &= 2\pi \int_0^{+\infty} d\omega \rho_{Dj}(\omega) |f_j(\omega)|^2 N(\omega, T) \\ &\quad \times [\delta(\omega + \omega') + \delta(\omega - \omega')], \\ \gamma_{j0}(\omega') &= 2\pi \int_0^{+\infty} d\omega \rho_{Dj}(\omega) |f_j(\omega)|^2 \delta(\omega - \omega'), \\ f_j(\omega) &= \begin{cases} g_1(\omega) & \text{if } j = 1, \\ \kappa(\omega) & \text{if } j = 2 \end{cases} \end{aligned} \quad (90)$$

and δ the Dirac-delta function.

Observe that the term multiplied by γ_{00} on the righthand side of the dissipator in (85) does not lead to a decay of the populations of the eigenstates $|\omega_n, \pm\rangle$ of \hat{H}_{DL} but it does lead to a decay of the coherences because its matrix elements between $|\omega_n, +\rangle$ and $|\omega_m, -\rangle$ can be different from zero. Physically, $\gamma_j(\omega')$ is associated with rates of stimulated and absorptive transitions at frequency ω' induced by B_j thermal excitations (photons if B_j is an electromagnetic field), while $\gamma_{j0}(\omega')$ is associated with rates of spontaneous transitions at frequency ω' induced by B_j . Since the qubit has degenerate energy levels, γ_{00} is associated with transition rates at frequency $\omega' = 0$.

It is important to note that \hat{b} and \hat{b}^\dagger are the annihilation and creation operators of a harmonic oscillator with the eigenvectors $|\omega_n, \pm\rangle$ of \hat{H}_{DL} in (40) playing the role of the number states, since

$$\begin{aligned} [\hat{b}, \hat{b}^\dagger] &= 1, \quad \hat{b}^\dagger |\omega_n, \pm\rangle = \sqrt{n+1} |\omega_{n+1}, \pm\rangle, \\ \hat{b}^\dagger \hat{b} |\omega_n, \pm\rangle &= n |\omega_n, \pm\rangle, \quad \hat{b} |\omega_n, \pm\rangle = \sqrt{n} |\omega_{n-1}, \pm\rangle. \end{aligned} \quad (91)$$

Not taking into account the term multiplied by γ_{00} in (85) and the driving on the right-hand side of (84), the master equation in (84) and (85) has the same form as the Born-Markov-secular master equation of a damped harmonic oscillator with \hat{b} and \hat{b}^\dagger as its annihilation and creation operators [52,53].

Observe that a stationary solution of (84) and (85) is given by the thermal state at frequency Ω (not Ω') of a harmonic

oscillator:

$$\hat{\rho}_{\text{SF}}^{ss} = \frac{1}{2} [1 - e^{-\hbar\Omega/(k_B T)}] \exp\left(-\frac{\hbar\Omega}{k_B T} \hat{b}^\dagger \hat{b}\right). \quad (92)$$

In the rest of the paper we assume that $\gamma_{00} = 0$ and that the temperature T of the thermal baths is sufficiently low so that $N(\Omega, T) \simeq 0$. Then, one can approximate the master equation (84) and (85) by the zero-temperature master equation

$$\frac{d}{dt} (\hat{\rho}_{\text{SF}})_I(t) = \mathcal{L}(\hat{\rho}_{\text{SF}})_I(t), \quad (93)$$

where the superoperator \mathcal{L} is defined by

$$\mathcal{L}\hat{\rho} = -\frac{i}{\hbar} [\hbar\Omega' \hat{b}^\dagger \hat{b}, \hat{\rho}] + \gamma_0 \hat{b} \hat{\rho} \hat{b}^\dagger - \frac{\gamma_0}{2} \{\hat{b}^\dagger \hat{b}, \hat{\rho}\}. \quad (94)$$

We have written (93) and (94) in the IP defined by the unitary transformation $\hat{U}_{IS}(t)$ in (22) to eliminate the driving term $-\hbar\Omega_d \cos(\omega_d t) \hat{\sigma}_x$ and to obtain a master equation with the same form as the zero-temperature master equation for a damped harmonic oscillator [52,53].

Note that the assumption $\gamma_{00} = 0$ is reasonable because it is associated with transition rates at frequency $\omega' = 0$. Sufficient mathematical requirements for this are the following: if $\rho_{Dj}(\omega) |f_j(\omega)|^2 \sim c_j \omega^{n_j}$ or $\rho_{Dj}(\omega) |f_j(\omega)|^2 \ll c_j \omega^{n_j}$ as $\omega \rightarrow 0^+$ for some constants $c_j > 0$ and $n_j > 1$ ($j = 1, 2$) with $f_j(\omega)$ in (90), then $\gamma_j(0) = \gamma_{j0}(0) = 0$ ($j = 1, 2$) and $\gamma_{00} = 0$. For example, a radiatively damped two-level atom satisfies this with $n = 3$ [53].

We now determine the evolution of some special states.

1. Separable states

Assume that the initial state of $S + F$ is a separable state where the qubit is in an eigenstate of $\hat{\sigma}_x$, that is, the initial state is of the form

$$\hat{\rho}_{\text{SF}}(0) = |\pm\rangle_{xx} \langle \pm| \otimes \hat{\rho}_F(0). \quad (95)$$

It follows from the master equation in (93) that the state of the system will always be separable and that the qubit will remain in the eigenstate of $\hat{\sigma}_x$. In addition, the IP and SP density operators are the same because the IP unitary transformation in (22) only affects the qubit and is given by a superposition of projectors onto the $|\pm\rangle_x$ states. Explicitly, the state of the system is

$$\hat{\rho}_{\text{SF}}(t) = |\pm\rangle_{xx} \langle \pm| \otimes \hat{\rho}_F(t), \quad (96)$$

where $\hat{\rho}_F(t)$ is given by

$$\hat{\rho}_F(t) = \hat{D}\left(\pm \frac{g}{\Omega}\right) \hat{\rho}_{\text{HO}}(t) \hat{D}^\dagger\left(\pm \frac{g}{\Omega}\right) \quad (97)$$

and $\hat{\rho}_{\text{HO}}(t)$ is the solution of the usual damped harmonic oscillator master equation at zero temperature [52]:

$$\begin{aligned} \frac{d}{dt} \hat{\rho}_{\text{HO}}(t) &= -\frac{i}{\hbar} [\hbar\Omega' \hat{a}^\dagger \hat{a}, \hat{\rho}_{\text{HO}}(t)] + \gamma_0 \hat{a} \hat{\rho}_{\text{HO}}(t) \hat{a}^\dagger \\ &\quad - \frac{\gamma_0}{2} \{\hat{a}^\dagger \hat{a}, \hat{\rho}_{\text{HO}}(t)\}, \end{aligned} \quad (98)$$

with the initial condition

$$\hat{\rho}_{\text{HO}}(0) = \hat{D}^\dagger\left(\pm \frac{g}{\Omega}\right) \hat{\rho}_F(0) \hat{D}\left(\pm \frac{g}{\Omega}\right). \quad (99)$$

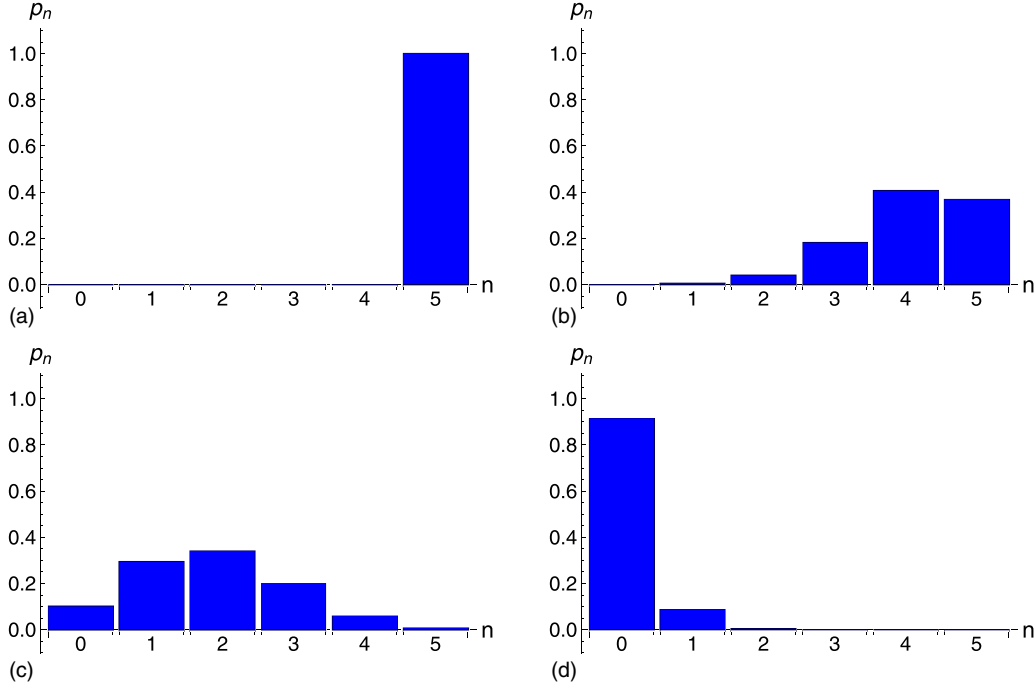


FIG. 3. Probabilities $p_n(t)$ in (103) as a function of n for $N = 5$ and the times $\gamma_0 t = 0$ (a), $1/5$ (b), 1 (c), and 4 (d).

There are two important cases where the initial state is separable and of the form (95), namely, the eigenvectors of \hat{H}_{DL} and the Schrödinger cat states in (55) above. We consider these now.

First assume that the initial state of $S + F$ is an eigenstate of \hat{H}_{DL} , that is,

$$\hat{\rho}_{SF}(0) = |\omega_N, \pm\rangle\langle\omega_N, \pm|. \quad (100)$$

From the evolution operator in (46) observe that, if there were no dissipation, then the system would remain in this state. Moreover, recall that $|\omega_N, \pm\rangle$ is an eigenvector of \hat{H}_{DL} with energy (eigenvalue) $\hbar\omega_N$ in (42). In particular, $|\omega_0, \pm\rangle$ have the smallest energies.

Note that (100) can be expressed in the form given in (95) by using the definition of the states $|\omega_n, \pm\rangle$ in (40):

$$\hat{\rho}_{SF}(0) = |\pm\rangle_{xx}\langle\pm| \otimes \hat{D}\left(\pm\frac{g}{\Omega}\right)|N\rangle\langle N|\hat{D}^\dagger\left(\pm\frac{g}{\Omega}\right). \quad (101)$$

It then follows that the state of $S + F$ at time t is

$$\hat{\rho}_{SF}(t) = \sum_{n=0}^N p_n(t) |\omega_n, \pm\rangle\langle\omega_n, \pm|, \quad (102)$$

with

$$p_n(t) = \frac{N!}{(N-n)!n!} (1 - e^{-\gamma_0 t})^{N-n} e^{-n\gamma_0 t}. \quad (103)$$

See Appendix C for the details of the calculation. In particular, observe that

$$p_N(t) = e^{-N\gamma_0 t}, \quad (104)$$

so the lifetime of the state (100) is $\gamma_0 t \sim 1/N$. Then, the larger the associated energy $\hbar\omega_N$ of (100), the smaller its lifetime. Also, $p_n(t)$ with $1 \leq n \leq N-1$ is maximized when $\gamma_0 t = \ln(N/n)$, so $\hat{\rho}_{SF}(t)$ quickly becomes a statistical mixture because $p_{N-1}(t)$ and $p_{N-2}(t)$ are rapidly maximized.

Figure 3 illustrates a typical evolution of the probabilities $p_n(t)$ in (103) for $N = 5$ and the times $\gamma_0 t = 0$ [Fig. 3(a)], $1/5$ [Fig. 3(b)], 1 [Fig. 3(c)], and 4 [Fig. 3(d)]. Observe that $\hat{\rho}_{SF}(0)$ starts as the pure state $|\omega_5, \pm\rangle\langle\omega_5, \pm|$ [Fig. 3(a)]. Then, it quickly becomes a mixed state involving non-negligible contributions $p_n(t)$ from several states $|\omega_n, \pm\rangle\langle\omega_n, \pm|$ after $\gamma_0 t = 1/5$ [Fig. 3(b)]. As time advances [Fig. 3(c)], the values of the n 's of the $|\omega_n, \pm\rangle\langle\omega_n, \pm|$ having non-negligible contributions in the statistical mixture decrease and $\hat{\rho}_{SF}(t)$ tends to the pure state $|\omega_0, \pm\rangle\langle\omega_0, \pm|$ [Fig. 3(d)]. Note that the latter is an eigenstate of \hat{H}_{DL} with minimum energy.

Now assume that $\hat{\rho}_{SF}(0)$ is a state of the form (95) with $\hat{\rho}_F(0)$ a pure state consisting of a superposition of coherent states, that is,

$$\hat{\rho}_F(0) = |\psi(0)\rangle\langle\psi(0)|, \quad (105)$$

with

$$|\psi(0)\rangle = \frac{1}{\mathcal{N}} (|\gamma_{10}\rangle + e^{i\chi} |\gamma_{20}\rangle), \quad (106)$$

$\gamma_{10} \neq \gamma_{20}$ complex numbers, χ a real number, and $\mathcal{N} > 0$ a normalization factor. Observe that the Schrödinger cat states $(1/N_\pm)|\xi(0)\rangle$ in (55) and (57)–(60) have this form if one chooses $n = 0$ in those equations.

Then, the state of $S + F$ at time t is given by (96) with

$$\begin{aligned} \hat{\rho}_F(t) = & \frac{1}{\mathcal{N}^2} \left[\left| \gamma_1(t) \pm \frac{g}{\Omega} \right\rangle \left\langle \gamma_1(t) \pm \frac{g}{\Omega} \right| \right. \\ & + \left| \gamma_2(t) \pm \frac{g}{\Omega} \right\rangle \left\langle \gamma_2(t) \pm \frac{g}{\Omega} \right| \\ & + f(t) \left| \gamma_1(t) \pm \frac{g}{\Omega} \right\rangle \left\langle \gamma_2(t) \pm \frac{g}{\Omega} \right| \\ & \left. + f(t)^* \left| \gamma_2(t) \pm \frac{g}{\Omega} \right\rangle \left\langle \gamma_1(t) \pm \frac{g}{\Omega} \right| \right], \quad (107) \end{aligned}$$

where

$$\begin{aligned}\gamma_j(t) &= \left(\gamma_{j0} \mp \frac{g}{\Omega}\right) e^{-(\gamma_0/2 + i\Omega')t}, \quad (j = 1, 2), \\ f(t) &= e^{-i\chi} \left\langle \gamma_{20} \mp \frac{g}{\Omega} \middle| \gamma_{10} \mp \frac{g}{\Omega} \right\rangle^{1-e^{-\gamma_0 t}} e^{-i\phi(t)},\end{aligned}\quad (108)$$

and

$$\phi(t) = \text{Im} \left\{ \pm \frac{g}{\Omega} (\gamma_{10} - \gamma_{20})^* [1 - e^{-(\gamma_0/2 - i\Omega')t}] \right\}.\quad (109)$$

See Appendix D for the details of the calculation.

The first thing to observe from (107)–(109) is that

$$\hat{\rho}_F(t) \rightarrow \left| \pm \frac{g}{\Omega} \right\rangle \left\langle \pm \frac{g}{\Omega} \right|, \quad (t \rightarrow +\infty).\quad (110)$$

Hence, instead of tending to the ground state $|0\rangle$, the state of the harmonic oscillator tends to the coherent state $|\pm g/\Omega\rangle$. We note that this effect is due to the coupling to the qubit and not to the driving. In particular, observe that the complex numbers $\gamma_1(t) \pm g/\Omega$ and $\gamma_2(t) \pm g/\Omega$ that appear as the arguments of the coherent states comprising $\hat{\rho}_F(t)$ in (107) spiral towards $\pm g/\Omega$. One can use this result to visualize what happens to the Schrödinger cat states $|\xi(0)\rangle$ given in (57)–(60) with $n = 0$. Assuming that the cat states $|\xi(0)\rangle$ have been prepared, the arguments of the displacement operators in $|\xi(0)\rangle$ and illustrated in Fig. 1 spiral clockwise towards the centers $\pm g/\Omega$ of their respective circles.

Substituting (110) in (96) and using the definition of the states $|\omega_n, \pm\rangle$ in (40), it follows that

$$\hat{\rho}_{\text{SF}}(t) \rightarrow |\omega_0, \pm\rangle \langle \omega_0, \pm| \quad (t \rightarrow +\infty),\quad (111)$$

so the system tends to an eigenstate of \hat{H}_{DL} with minimum energy.

To determine the lifetime of the superposition of coherent states in (105) and (106), one must determine the decoherence time (the time over which coherences are destroyed). From (107) the decoherence function is

$$\Gamma(t) = \ln|f(t)| = -\frac{1}{2}|\gamma_{10} - \gamma_{20}|^2(1 - e^{-\gamma_0 t}).\quad (112)$$

Making a linear approximation in $\gamma_0 t$ in (112) one gets

$$\Gamma(t) = -\frac{1}{2}|\gamma_{10} - \gamma_{20}|^2(\gamma_0 t),\quad (113)$$

so the decoherence time is

$$t_D = \frac{2}{\gamma_0 |\gamma_{10} - \gamma_{20}|^2}.\quad (114)$$

Assuming that the cat states $|\xi(0)\rangle$ in (57)–(60) with $n = 0$ have been prepared, one can use this result to determine their lifetime. For all the Schrödinger cat states in (57)–(60)

$$t_D = \frac{1}{8\gamma_0 |g/\Omega|^2}.\quad (115)$$

The decoherence time is inversely proportional to the square of the coupling. Hence, the larger the coupling $|g/\Omega|$, the shorter the lifetime so USC values of $|g/\Omega|$ are preferable over DSC values. In particular, it is convenient to have $|g/\Omega| \sim 0.537$ because one would have an easily discernible (the overlap of the states composing the cat state is ≤ 0.01), long-lived cat state with $t_D \sim 0.43/\gamma_0$.

2. Nonseparable states

In this section we discuss the evolution of some nonseparable states of $S + F$ that start as pure states:

$$\hat{\rho}_{\text{SF}}(0) = |\psi(0)\rangle \langle \psi(0)|.\quad (116)$$

First, assume that both the qubit and the harmonic oscillator are initially in their respective ground states, that is, the initial state of the system is (61). Solving the master equation in (93) for the initial condition (116) with (61), one finds that the state of $S + F$ evolves as

$$\begin{aligned}\hat{\rho}_{\text{SF}}(t) &= \frac{1}{2} \left[|+\rangle_{xx} \langle +| \otimes \left| -\gamma_1(t) + \frac{g}{\Omega} \right\rangle \left\langle -\gamma_1(t) + \frac{g}{\Omega} \right| \right. \\ &\quad + F(t) |+\rangle_{xx} \langle -| \otimes \left| -\gamma_1(t) + \frac{g}{\Omega} \right\rangle \left\langle \gamma_1(t) - \frac{g}{\Omega} \right| \\ &\quad + F(t)^* |-\rangle_{xx} \langle +| \otimes \left| \gamma_1(t) - \frac{g}{\Omega} \right\rangle \left\langle -\gamma_1(t) + \frac{g}{\Omega} \right| \\ &\quad \left. + |-\rangle_{xx} \langle -| \otimes \left| \gamma_1(t) - \frac{g}{\Omega} \right\rangle \left\langle \gamma_1(t) - \frac{g}{\Omega} \right| \right],\end{aligned}\quad (117)$$

with

$$\begin{aligned}\gamma_1(t) &= \frac{g}{\Omega} e^{-(\gamma_0/2 + i\Omega')t}, \\ F(t) &= -\exp\left[i\theta(t_1) - 2\left|\frac{g}{\Omega}\right|^2(1 - e^{-\gamma_0 t})\right].\end{aligned}\quad (118)$$

See Appendix D for the details of the calculation, where the evolution of a more general type of state is presented.

Result (117) allows one to determine under which conditions one can still create the Schrödinger cat state in (69). One simply requires (117) to be approximately equal to $|\psi(t)\rangle \langle \psi(t)|$ with $|\psi(t)\rangle$ the state of $S + F$ in (62) when there is no dissipation. This happens if $\pi/\Omega' \ll 1/\gamma_0$ or, equivalently, if the decay rate γ_0 is much smaller than the shifted harmonic oscillator frequency Ω' . Also note that the times T_n in (66) have to be changed to $T_n = (2n - 1)\pi/\Omega'$ to take into account the small frequency shift of Ω .

The probability to find the qubit in the excited state suffers an interesting change. It is given by

$$\begin{aligned}P_2(t) &= \frac{1}{2} - \frac{1}{2} \cos[\theta(t_1)] \\ &\quad \times \exp\left\{-4\left|\frac{g}{\Omega}\right|^2 [1 - \cos(\Omega' t) e^{-\gamma_0 t/2}]\right\}.\end{aligned}\quad (119)$$

Comparing (74) with (119), one finds that the differences are the presence of the exponential $e^{-\gamma_0 t/2}$ and the shifted harmonic oscillator frequency Ω' . Hence, the effect of the thermal baths is to decrease the maximum value of $P_2(t)$ and to increase its minimum value. In particular, if $|g/\Omega| \geq 1$, then $P_2(t)$ approximately tends to the value $1/2$, as illustrated in Fig. 4. The probability behaves in this way because the state of $S + F$ approximately tends to the maximum mixed state composed of the eigenstates of \hat{H}_{DL} with minimum energy if $|g/\Omega| \geq 1$:

$$\hat{\rho}_{\text{SF}}(t) \rightarrow \frac{1}{2} [|\omega_0, +\rangle \langle \omega_0, +| + |\omega_0, -\rangle \langle \omega_0, -|].\quad (120)$$

Note that $|\omega_0, \pm\rangle$ is an equal weights superposition involving the states $|1\rangle$ and $|2\rangle$, so $P_2(t)$ tends to $1/2$ if $|g/\Omega| \geq 1$.

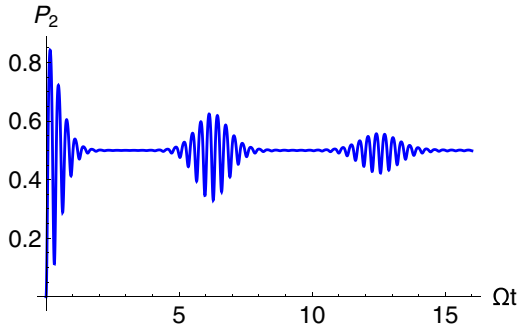


FIG. 4. $P_2(t)$ in (119) as a function of Ωt for the values in (79) and $\gamma_0/\Omega = 0.1$. Compare with Fig. 2(b).

Finally, consider an initial state of the form (116) with

$$|\psi(0)\rangle = \frac{1}{\sqrt{2}}(|\omega_0, +\rangle + e^{i\chi}|\omega_0, -\rangle), \quad (121)$$

and χ a real number. Notice that $|\psi(0)\rangle$ is a superposition of the eigenstates of \hat{H}_{DL} with minimum energy and that $\hat{\rho}_{SF}(0)$ is a stationary state of the master equation in (93). Using the unitary transformation $\hat{U}_{IS}(t)$ in (22) to change $(\hat{\rho}_{SF})_I(t) = \hat{\rho}_{SF}(0)$ back to the SP, one finds that the state of $S + F$ is a pure state given by

$$|\psi(t)\rangle = \frac{1}{2}|2\rangle \otimes \left\{ \left| \frac{g}{\Omega} \right\rangle + e^{-i[\theta(t_1) - \chi]} \left| -\frac{g}{\Omega} \right\rangle \right\} + \frac{1}{2}|1\rangle \otimes \left\{ \left| \frac{g}{\Omega} \right\rangle - e^{-i[\theta(t_1) - \chi]} \left| -\frac{g}{\Omega} \right\rangle \right\}. \quad (122)$$

Hence, the state of $S + F$ evolves into a stable superposition that involves Schrödinger cat states of the harmonic oscillator. To have easily discernible cat states one needs DSC values $|g/\Omega| \geq 1$ so that $|(g/\Omega) - (g/\Omega)|^2 < 0.02$. For these values of the coupling, the probability to find the qubit in the excited state $|2\rangle$ is approximately equal to $1/2$. These highly entangled states are robust against dissipation and could be used for quantum information processes.

D. The case $B_1 = B_2$

In all the above it was assumed that B_1 and B_2 are two independent thermal baths to which the open system $S + F$ is coupled. Recall that only S is coupled to B_1 and that only F is coupled to B_2 . The purpose of this section is to answer the following question: What happens if $B_1 = B_2$, that is, what happens if B_1 and B_2 are the same thermal bath?

If $B_1 = B_2$, then the following changes occur. First, \hat{H}_{B_2} and $\hat{\rho}_{B_2}(0)$ must be eliminated wherever they appear and \hat{a}_{2k} must be replaced by \hat{a}_{1k} everywhere. Second, since the IP unitary transformation $\hat{U}_{IS}(t)$ only affects operators of S , all the steps leading to the IP von Neumann equation (26) hold. Now, the averaging only affects the vector $\hat{\mathbf{u}}(t_1)$ and leaves all the operators unaffected because they are time independent. Hence, all the steps leading to the averaged von Neumann IP equation in (31) also hold. We emphasize that this happens because the IP unitary transformation only affects the qubit and the averaging only affects the vector $\hat{\mathbf{u}}(t_1)$.

Finally, the density of states $\rho_{D2}(\omega)$ has to be replaced everywhere by $\rho_{D1}(\omega)$ and one obtains exactly the same master equation in (84) and (85) except that the decay rate γ_{00} has to be replaced by

$$\gamma_{000} = \gamma_{00} + \gamma_{12}(0) \left(\frac{g + g^*}{\Omega} \right), \quad (123)$$

with γ_{00} in (89) and

$$\gamma_{12}(\omega') = 2\pi \int_0^{+\infty} d\omega \delta(\omega - \omega') \rho_{D1}(\omega) [2N(\omega, T) + 1] \times [g_1(\omega)^* \kappa(\omega) + g_1(\omega) \kappa(\omega)^*]. \quad (124)$$

Hence, $B_1 = B_2$ only modifies a single decay rate.

VI. CONCLUSIONS

In this paper we considered the quantum Rabi model as an open system that is subject to dissipation, dephasing, and sinusoidal qubit driving. It was shown that one can change to an interaction picture where the qubit-driving term disappears at the expense of changing the free energy of the qubit which becomes time dependent. Now, if the qubit-driving frequency is large with respect to the rest of the parameters with the exception of the qubit-driving strength, then one can obtain an effective interaction picture Hamiltonian that accurately describes the dynamics of the qubit-harmonic oscillator system and where the driving has two effects: the qubit-transition frequency is changed and the qubit has reduced dephasing. The qubit-driving strength can be chosen so that the qubit-transition frequency is reduced, made equal to zero, or even made negative so that the excited and ground states of the qubit are interchanged. Therefore, sinusoidal qubit driving offers another method to control the qubit-transition frequency and to reduce qubit dephasing. In particular, initially quasiresonant qubit-harmonic oscillator interactions can be made nonresonant and vice versa.

Adjusting the qubit-driving strength allows one to consider a qubit with degenerate energy levels. Not taking dissipation into account, it was found that the evolution operator of the qubit-harmonic oscillator system is given by a linear combination of the orthogonal projectors onto the eigenstates of $\hat{\sigma}_x$ followed by the evolution operator of a forced harmonic oscillator. This was used to show that the harmonic oscillator can be prepared in such a way that it is always found in a Schrödinger cat state. This is particularly relevant to quantum information where these states have been used for quantum error correction [39]. Also, the transition probability of the qubit can exhibit a collapse-revival behavior. In addition, the Born-Markov-secular master equation was deduced and the effects of dissipation were presented. In particular, it was found that smaller ultrastrong-coupling values are preferable over larger ultrastrong-coupling values and deep strong-coupling values in order to have long-lived, easily distinguishable Schrödinger cat states because the decoherence rate is inversely proportional to the square of the coupling. Finally, it was shown that the qubit-harmonic oscillator system can be prepared in highly entangled states that are stable under dissipation and that could be used in quantum information processes.

The results are especially useful in the area of circuit quantum electrodynamics and cold atoms where the ultrastrong-coupling regime can be reached. In particular, ultrastrong coupling is required to have easily distinguishable, long-lived Schrödinger cat states. It would be very interesting to apply the results to the cold atom system of [29] because it has very small dissipation, it can be described by the quantum Rabi model, and the harmonic oscillator consists of the degrees of motion of an atom. Hence, the atom could be prepared in a Schrödinger cat state where it is found in a superposition of two different positions. Finally, the results can also be applied to atomic systems such as that involving lithium 6 in [45,46] where the two-level approximation is very accurate in spite of having a large driving strength and frequency. Nevertheless, these types of systems usually cannot reach the ultrastrong-coupling regime.

APPENDIX A: AVERAGING OF VON NEUMANN'S IP EQUATION

To derive the averaged equation it is convenient to use nondimensional quantities. Define

$$\tau = \omega_d t, \quad \tilde{\rho}_I(\tau) = \hat{\rho}_I\left(\frac{\tau}{\omega_d}\right). \quad (\text{A1})$$

Notice that τ is the nondimensional time and that

$$t_1 = \tau, \quad t_2 = \left(\frac{\omega_s - \delta_3}{\omega_d}\right)\tau. \quad (\text{A2})$$

Then, von Neumann's IP equation (26) takes the form

$$\frac{d}{d\tau} \tilde{\rho}_I(\tau) = -i \left[\frac{1}{\hbar\omega_d} \hat{H}_I(\tau), \tilde{\rho}_I(\tau) \right]. \quad (\text{A3})$$

Observe from (27) and (30) that each term of $\hat{H}_I(\tau)/(\hbar\omega_d)$ is multiplied by a very small quantity and that the only τ dependence of $\hat{H}_I(\tau)/(\hbar\omega_d)$ comes from $\hat{\mathbf{u}}(\tau)$. Moreover, observe from (23) and (28) that $\hat{\mathbf{u}}(\tau)$ is τ periodic with period 2π . Hence, it follows from (A3) that $\tilde{\rho}_I(\tau)$ evolves slowly, while $\hat{H}_I(\tau)/(\hbar\omega_d)$ evolves rapidly and is 2π periodic. Then,

$$\tilde{\rho}_I(\tau') \simeq \tilde{\rho}_I(\tau) \quad \text{for all } \tau' \in [\tau, \tau + 2\pi], \quad (\text{A4})$$

and

$$\frac{d\tilde{\rho}_I}{d\tau}(\tau) \simeq \frac{\tilde{\rho}_I(\tau + 2\pi) - \tilde{\rho}_I(\tau)}{2\pi}. \quad (\text{A5})$$

Integrating (A3) in the interval $[\tau, \tau + 2\pi]$ and using (A4) and (A5) one gets

$$\begin{aligned} \frac{d}{d\tau} \tilde{\rho}_I(\tau) &\simeq -\frac{i}{2\pi} \int_{\tau}^{\tau+2\pi} d\tau' \left[\frac{1}{\hbar\omega_d} \hat{H}_I(\tau'), \tilde{\rho}_I(\tau) \right] \\ &= -\frac{i}{\hbar\omega_d} [\hat{H}_I^{\text{avg}}, \tilde{\rho}_I(\tau)], \end{aligned} \quad (\text{A6})$$

with the averaged Hamiltonian

$$\hat{H}_I^{\text{avg}} = \frac{1}{2\pi} \int_{\tau}^{\tau+2\pi} d\tau' \hat{H}_I(\tau'). \quad (\text{A7})$$

This Hamiltonian reduces to (32) once one substitutes $\hat{H}_I(\tau)$ given in (27) and one applies Bessel's integral formulas [47].

Using (A1) to introduce units, it follows from (A6) that the averaged equation for $\hat{\rho}_I(t)$ is given in (31) where we have added the superscript *avg* to indicate that it is the averaged equation.

APPENDIX B: PROPERTIES OF THE DISPLACEMENT OPERATOR

Some properties of the displacement operator that are used throughout the main text are the following:

$$\begin{aligned} \hat{a}|\gamma\rangle &= \gamma|\gamma\rangle, \quad e^{-i\Omega\hat{a}^\dagger\hat{a}t} \hat{D}(\gamma)|0\rangle = |\gamma e^{-i\Omega t}\rangle, \\ \hat{D}^\dagger(\gamma) &= \hat{D}(-\gamma), \quad e^{\gamma\hat{a}^\dagger\hat{a}} \hat{a} e^{-\gamma\hat{a}^\dagger\hat{a}} = e^{-\gamma} \hat{a}, \\ \hat{D}^\dagger(\gamma) \hat{a} \hat{D}(\gamma) &= \hat{a} + \gamma, \quad e^{\gamma\hat{a}^\dagger\hat{a}} \hat{a} e^{-\gamma\hat{a}^\dagger\hat{a}} = \hat{a} - \gamma, \\ [\hat{a}, \hat{D}(\gamma)] &= \gamma \hat{D}(\gamma), \quad \hat{D}(\gamma) \hat{a} \hat{D}(\gamma) = \hat{D}(2\gamma)(\hat{a} + \gamma), \end{aligned}$$

and

$$\begin{aligned} e^{\gamma_1\hat{a}^\dagger\hat{a}} \hat{D}(\gamma) e^{-\gamma_1\hat{a}^\dagger\hat{a}} &= \exp[(\gamma e^{\gamma_1})\hat{a}^\dagger - (\gamma^* e^{-\gamma_1})\hat{a}], \\ \hat{D}(\gamma_1) \hat{D}(\gamma_2) &= e^{\frac{1}{2}(\gamma_1\gamma_2^* - \gamma_1^*\gamma_2)} \hat{D}(\gamma_1 + \gamma_2), \\ \hat{D}^\dagger(\gamma) e^{-i\Omega\hat{a}^\dagger\hat{a}t} &= e^{-i\Omega\hat{a}^\dagger\hat{a}t} \hat{D}(-\gamma e^{i\Omega t}). \end{aligned} \quad (\text{B1})$$

Here $|0\rangle$ is the number state with $n = 0$ and γ , γ_1 , and γ_2 are complex numbers. These properties can be proved using the Baker-Campbell-Hausdorff formula [54] and the following result: if A and B are linear operators that commute with their commutator, then $[A, F(B)] = [A, B]F'(B)$ with $F(x)$ a function [49].

APPENDIX C: EVOLUTION OF $|\omega_N, \pm\rangle\langle\omega_N, \pm|$

In this Appendix we show how to determine the evolution of $|\omega_N, \pm\rangle\langle\omega_N, \pm|$ under the zero-temperature master equation in (93) and (94).

Assume that the initial state of $S + F$ is given by (100), that is, by $|\omega_N, \pm\rangle\langle\omega_N, \pm|$. Now, given that the $|\omega_n, \pm\rangle$ behave as number states for \hat{b} and \hat{b}^\dagger [see (91)], it follows from (94) that $\mathcal{L}|\omega_n, \pm\rangle\langle\omega_n, \pm|$ gives a linear combination of $|\omega_n, \pm\rangle\langle\omega_n, \pm|$ and $|\omega_{n-1}, \pm\rangle\langle\omega_{n-1}, \pm|$. Since \mathcal{L} only provokes decay from one $|\omega_n, \pm\rangle$ to another, this leads one to propose $\hat{\rho}_{\text{SF}}(t)$ in (102) as the state of $S + F$ at time t . Substituting (102) into the zero-temperature master equation (93) and (94), one obtains the following system of differential equations:

$$\frac{d}{dt} e^{\gamma_0 t} p_n(t) = \gamma_0(n+1) e^{-\gamma_0 t} [e^{\gamma_0(n+1)t} p_{n+1}(t)], \quad (\text{C1})$$

with $n = 0, 1, \dots, N$ and $p_{N+1}(t) = 0$. Solving system (C1) for the first few cases $n = N, N-1, N-2$, and $N-3$ leads one to propose formula (103) for $p_n(t)$, which can then be proved by induction. In addition, substituting $\hat{\rho}_{\text{SF}}(t)$ in (102) into the zero-temperature master equation (93) and using expression (103) for $p_n(t)$, one indeed finds that (102) and (103) is the solution of the master equation (93) for the initial condition in (100).

APPENDIX D: EVOLUTION OF SOME NONSEPARABLE STATES

In this Appendix we present how to determine the evolution of certain nonseparable states presented in the main

text. In order to do this, we first define coherent states of the annihilation operator \hat{b} .

It was observed in (91) that the operators \hat{b}^\dagger and \hat{b} are the creation and annihilation operators of a harmonic oscillator where the states $|\omega_n, \pm\rangle$ take the place of the number states. Then, one can define coherent states $|\gamma, \pm\rangle$ of \hat{b} as follows:

$$|\gamma, \pm\rangle = e^{-\frac{1}{2}|\gamma|^2} \sum_{n=0}^{+\infty} \frac{\gamma^n}{\sqrt{n!}} |\omega_n, \pm\rangle, \quad (\text{D1})$$

where γ is any complex number. One can readily verify that the kets (D1) are normalized eigenvectors of \hat{b} :

$$\hat{b}|\gamma, \pm\rangle = \gamma|\gamma, \pm\rangle, \quad \langle\gamma, \pm|\gamma, \pm\rangle = 1. \quad (\text{D2})$$

The connection with the coherent states of F (eigenvectors of \hat{a}) can be established by using the definition of the states $|\omega_n, \pm\rangle$ in (40):

$$|\gamma, \pm\rangle = e^{\pm(g\gamma^* - g^*\gamma)/(2\Omega)} |\pm\rangle_x \otimes \left| \gamma \pm \frac{g}{\Omega} \right\rangle. \quad (\text{D3})$$

Then, except for a global phase, the coherent states $|\gamma, \pm\rangle$ of \hat{b} are the tensor product of an eigenstate of $\hat{\sigma}_x$ with a coherent state of F .

Now we are going to determine how superpositions of coherent states of \hat{b} evolve under the zero-temperature master equation (93).

Assume that the initial state of the system is the pure state in (116) with $|\psi(0)\rangle$ the following superposition of coherent states of \hat{b} :

$$|\psi(0)\rangle = \frac{1}{\sqrt{2}} (|\gamma_{10}, +\rangle + e^{i\chi} |\gamma_{20}, -\rangle). \quad (\text{D4})$$

Here γ_{10} and γ_{20} are complex numbers, while χ is a real number.

Using the superoperator \mathcal{L} defined in (94), the solution of the zero-temperature master equation (93) can be written as

$$(\hat{\rho}_{\text{SF}})_I(t) = e^{\mathcal{L}t} \hat{\rho}_{\text{SF}}(0), \quad (\text{D5})$$

where we have used that the IP and SP coincide at time $t = 0$ [see (22) and (25)].

Since $e^{\mathcal{L}t}$ is a linear superoperator and $\hat{\rho}_{\text{SF}}(0) = |\psi(0)\rangle\langle\psi(0)|$ with $|\psi(0)\rangle$ given in (D4), to calculate $(\hat{\rho}_{\text{SF}})_I(t)$ in (D5) one only needs to calculate

$$e^{\mathcal{L}t} |\alpha_{10}, j\rangle\langle\alpha_{20}, k|, \quad (\text{D6})$$

where $j, k \in \{+, -\}$ and $|\alpha_{10}, j\rangle$ and $|\alpha_{20}, k\rangle$ are arbitrary coherent states of \hat{b} . Therefore, consider the initial state

$$|\alpha_{10}, j\rangle\langle\alpha_{20}, k|, \quad (\text{D7})$$

and propose that it evolves under the zero-temperature master equation (93) as

$$\sigma(t) = e^{\mathcal{L}t} |\alpha_{10}, j\rangle\langle\alpha_{20}, k| = f(t) |\alpha_1(t), j\rangle\langle\alpha_2(t), k| \quad (\text{D8})$$

with $f(t)$ a complex-valued function. In order to satisfy the initial condition (D7) it must happen that

$$\alpha_l(0) = \alpha_{l0}, \quad (l = 1, 2), \quad f(0) = 1. \quad (\text{D9})$$

Substituting (D8) in the master equation (93), one finds that

$$\begin{aligned} & \left[\frac{f'(t)}{f(t)} - \frac{1}{2} \frac{d}{dt} |\alpha_1(t)|^2 - \frac{1}{2} \frac{d}{dt} |\alpha_2(t)|^2 \right] \sigma(t) \\ & + \frac{\alpha_1'(t)}{\alpha_1(t)} \hat{b}^\dagger \hat{b} \sigma(t) + \left[\frac{\alpha_2'(t)}{\alpha_2(t)} \right]^* \sigma(t) \hat{b}^\dagger \hat{b} \\ & = \gamma_0 \alpha_1(t) \alpha_2(t)^* \sigma(t) - \left(\frac{\gamma_0}{2} + i\Omega' \right) \hat{b}^\dagger \hat{b} \sigma(t) \\ & - \left(\frac{\gamma_0}{2} - i\Omega' \right) \sigma(t) \hat{b}^\dagger \hat{b}. \end{aligned} \quad (\text{D10})$$

Equating the coefficients of $\sigma(t)$, $\hat{b}^\dagger \hat{b} \sigma(t)$, and $\sigma(t) \hat{b}^\dagger \hat{b}$ and solving the resulting equations, one finds that (D8) is a solution of (93) that satisfies the initial conditions (D9) if and only if

$$\begin{aligned} \alpha_l(t) &= \alpha_{l0} e^{-(\gamma_0/2 + i\Omega')t}, \quad (l = 1, 2), \\ f(t) &= \langle\alpha_{20}|\alpha_{10}\rangle^{1 - e^{-\gamma_0 t}}, \end{aligned} \quad (\text{D11})$$

where $|\alpha_{10}\rangle$ and $|\alpha_{20}\rangle$ are coherent states of F .

Using the results (D8) and (D11) in (D5), one obtains

$$\begin{aligned} (\hat{\rho}_{\text{SF}})_I(t) &= \frac{1}{2} [|+\rangle_{xx} \langle +| + |\gamma_2(t), -\rangle \langle \gamma_2(t), -| \\ & + F_1(t) |+\rangle_{xx} \langle +| + |\gamma_2(t), -\rangle \langle \gamma_2(t), -| \\ & + F_1(t)^* |-\rangle_{xx} \langle -| + |\gamma_1(t), +\rangle \langle \gamma_1(t), +|], \end{aligned} \quad (\text{D12})$$

with

$$\begin{aligned} \gamma_l(t) &= \gamma_{l0} e^{-(\gamma_0/2 + i\Omega')t}, \quad (l = 1, 2), \\ F_1(t) &= e^{-i\chi} \langle\gamma_{20}|\gamma_{10}\rangle^{1 - e^{-\gamma_0 t}}. \end{aligned} \quad (\text{D13})$$

Using the connection with coherent states of F in (D3) and the unitary transformation $\hat{U}_{IS}(t)$ in (22) to change back to the SP, it follows from (D12) that

$$\begin{aligned} \hat{\rho}_{\text{SF}}(t) &= \frac{1}{2} \left[|+\rangle_{xx} \langle +| \otimes \left| \gamma_1(t) + \frac{g}{\Omega} \right\rangle \left\langle \gamma_1(t) + \frac{g}{\Omega} \right| \right. \\ & + F(t) |+\rangle_{xx} \langle -| \otimes \left| \gamma_1(t) + \frac{g}{\Omega} \right\rangle \left\langle \gamma_2(t) - \frac{g}{\Omega} \right| \\ & + |-\rangle_{xx} \langle -| \otimes \left| \gamma_2(t) - \frac{g}{\Omega} \right\rangle \left\langle \gamma_2(t) - \frac{g}{\Omega} \right| \\ & \left. + F(t)^* |-\rangle_{xx} \langle +| \otimes \left| \gamma_2(t) - \frac{g}{\Omega} \right\rangle \left\langle \gamma_1(t) + \frac{g}{\Omega} \right| \right]. \end{aligned} \quad (\text{D14})$$

Using $\theta(t_1)$ in (23), the quantities in (D13), and the imaginary part $\text{Im}(z)$ of a complex number z , $F(t)$ can be expressed as

$$F(t) = e^{i\theta(t)} F_1(t) \exp \left(i \text{Im} \left\{ \frac{g}{\Omega} [\gamma_1(t) + \gamma_2(t)]^* \right\} \right). \quad (\text{D15})$$

Now, the state $|1\rangle \otimes |0\rangle$ that describes the qubit and the harmonic oscillator in their respective ground states can be expressed in the form (D4) by choosing

$$\gamma_{10} = -\frac{g}{\Omega}, \quad \gamma_{20} = \frac{g}{\Omega}, \quad \chi = \pi. \quad (\text{D16})$$

Hence, the evolution of the state $|1\rangle \otimes |0\rangle$ under the zero-temperature master equation (93) can be obtained from (D13)–(D15) by using the values in (D16). This was presented in (117).

Finally, using exactly the same method presented above, one can calculate the evolution of superpositions of coherent states of F presented in (106) and (107).

-
- [1] D. Braak, Q.-H. Chen, M. T. Batchelor, and E. Solano, Semi-classical and quantum Rabi models: In celebration of 80 years, *J. Phys. A: Math. Theor.* **49**, 300301 (2016).
- [2] A. Eisfeld, L. Braun, W. T. Strunz, J. S. Briggs, J. Beck, and V. Engel, Vibronic energies and spectra of molecular dimers, *J. Chem. Phys.* **122**, 134103 (2005).
- [3] A. B. Klimov and S. M. Chumakov, *A Group-Theoretical Approach to Quantum Optics* (Wiley, New York, 2009).
- [4] T. Liu, K. L. Wang, and M. Feng, The generalized analytical approximation to the solution of the single-mode spin-boson model without rotating-wave approximation, *Europhys. Lett.* **86**, 54003 (2009).
- [5] V. V. Albert, G. D. Scholes, and P. Brumer, Symmetric rotating-wave approximation for the generalized single-mode spin-boson system, *Phys. Rev. A* **84**, 042110 (2011).
- [6] S. Ashhab and F. Nori, Qubit-oscillator systems in the ultrastrong-coupling regime and their potential for preparing nonclassical states, *Phys. Rev. A* **81**, 042311 (2010).
- [7] J. Hausinger and M. Grifoni, Qubit-oscillator system: An analytical treatment of the ultrastrong coupling regime, *Phys. Rev. A* **82**, 062320 (2010).
- [8] H. Walther, B. T. H. Varcoe, B. G. Englert, and T. Becker, Cavity quantum electrodynamics, *Rep. Prog. Phys.* **69**, 1325 (2006).
- [9] J. M. Raimond, M. Brune, and S. Haroche, Manipulating quantum entanglement with atoms and photons in a cavity, *Rev. Mod. Phys.* **73**, 565 (2001).
- [10] Z. L. Xiang, S. Ashhab, J. Q. You, and F. Nori, Hybrid quantum circuits: Superconducting circuits interacting with other quantum systems, *Rev. Mod. Phys.* **85**, 623 (2013).
- [11] X. Gu, A. F. Kockum, A. Miranowicz, and Y. X. Liu, Microwave photonics with superconducting quantum circuits, *Phys. Rep.* **718-719**, 1 (2017).
- [12] P. Forn-Díaz, L. Lamata, E. Rico, J. Kono, and E. Solano, Ultrastrong coupling regimes of light-matter interaction, *Rev. Mod. Phys.* **91**, 025005 (2019).
- [13] A. F. Kockum, A. Miranowicz, S. D. Liberato, S. Savasta, and F. Nori, Ultrastrong coupling between light and matter, *Nat. Rev. Phys.* **1**, 19 (2019).
- [14] D. Z. Rossatto, C. J. Villas-Bôas, M. Sanz, and E. Solano, Spectral classification of coupling regimes in the quantum rabi model, *Phys. Rev. A* **96**, 013849 (2017).
- [15] J. Casanova, G. Romero, I. Lizuain, J. J. García-Ripoll, and E. Solano, Deep Strong Coupling Regime of the Jaynes-Cummings Model, *Phys. Rev. Lett.* **105**, 263603 (2010).
- [16] E. K. Irish, J. Gea-Banacloche, I. Martin, and K. C. Schwab, Dynamics of a two-level system strongly coupled to a high-frequency quantum oscillator, *Phys. Rev. B* **72**, 195410 (2005).
- [17] D. Zueco, G. M. Reuther, S. Kohler, and P. Hänggi, Qubit-oscillator dynamics in the dispersive regime: Analytical theory beyond the rotating-wave approximation, *Phys. Rev. A* **80**, 033846 (2009).
- [18] E. K. Irish, Generalized Rotating-Wave Approximation for Arbitrarily Large Coupling, *Phys. Rev. Lett.* **99**, 173601 (2007).
- [19] L. Yu, S. Zhu, Q. Liang, G. Chen, and S. Jia, Analytical solutions for the Rabi model, *Phys. Rev. A* **86**, 015803 (2012).
- [20] M. Amnat-Talab, S. Guérin, and H. R. Jauslin, Quantum averaging and resonances: Two-level atom in a one-mode quantized field, *J. Math. Phys.* **46**, 042311 (2005).
- [21] D. Braak, Integrability of the Rabi Model, *Phys. Rev. Lett.* **107**, 100401 (2011).
- [22] Q.-H. Chen, C. Wang, S. He, T. Liu, and K.-L. Wang, Exact solvability of the quantum Rabi model using Bogoliubov operators, *Phys. Rev. A* **86**, 023822 (2012).
- [23] H. Zhong, Q. Xie, M. T. Batchelor, and C. Lee, Analytical eigenstates for the quantum Rabi model, *J. Phys. A: Math. Theor.* **46**, 415302 (2013).
- [24] A. J. Maciejewski, M. Przybylska, and T. Stachowiak, An exactly solvable system from quantum optics, *Phys. Lett. A* **379**, 1503 (2015).
- [25] P. Forn-Díaz, J. J. García-Ripoll, B. Peropadre, J.-L. Orgiazzi, M. A. Yurtalan, R. Belyansky, C. M. Wilson, and A. Lupascu, Ultrastrong coupling of a single artificial atom to an electromagnetic continuum in the nonperturbative regime, *Nat. Phys.* **13**, 39 (2017).
- [26] C. Maissen, G. Scalari, F. Valmorra, M. Beck, J. Faist, S. Cibella, R. Leoni, C. Reichl, C. Charpentier, and W. Wegscheider, Ultrastrong coupling in the near field of complementary split-ring resonators, *Phys. Rev. B* **90**, 205309 (2014).
- [27] A. Bayer, M. Pozimski, S. Schambeck, D. Schuh, R. Huber, D. Bougeard, and C. Lange, Terahertz light-matter interaction beyond unity coupling strength, *Nano Lett.* **17**, 6340 (2017).
- [28] F. Yoshihara, T. Fuse, S. Ashhab, K. Kakuyanagi, S. Saito, and K. Semba, Superconducting qubit-oscillator circuit beyond the ultrastrong-coupling regime, *Nat. Phys.* **13**, 44 (2017).
- [29] A. Dareau, Y. Meng, P. Schneeweiss, and A. Rauschenbeutel, Observation of Ultrastrong Spin-Motion Coupling for Cold Atoms in Optical Microtraps, *Phys. Rev. Lett.* **121**, 253603 (2018).
- [30] G. Romero, D. Ballester, Y. M. Wang, V. Scarani, and E. Solano, Ultrafast Quantum Gates in Circuit QED, *Phys. Rev. Lett.* **108**, 120501 (2012).
- [31] A. F. Kockum, V. Macri, L. Garziano, S. Savasta, and F. Nori, Frequency conversion in ultrastrong cavity QED, *Sci. Rep.* **7**, 5313 (2017).
- [32] D. Ballester, G. Romero, J. J. García-Ripoll, F. Deppe, and E. Solano, Quantum Simulation of the Ultrastrong-Coupling Dynamics in Circuit Quantum Electrodynamics, *Phys. Rev. X* **2**, 021007 (2012).
- [33] I. M. Georgescu, S. Ashhab, and F. Nori, Quantum simulation, *Rev. Mod. Phys.* **86**, 153 (2014).
- [34] C. Ciuti, G. Bastard, and I. Carusotto, Quantum vacuum properties of the intersubband cavity polariton field, *Phys. Rev. B* **72**, 115303 (2005).

- [35] R. Stassi, A. Ridolfo, O. Di Stefano, M. J. Hartmann, and S. Savasta, Spontaneous Conversion from Virtual to Real Photons in the Ultrastrong-Coupling Regime, *Phys. Rev. Lett.* **110**, 243601 (2013).
- [36] L. Garziano, V. Macrì, R. Stassi, O. Di Stefano, F. Nori, and S. Savasta, One Photon Can Simultaneously Excite Two or More Atoms, *Phys. Rev. Lett.* **117**, 043601 (2016).
- [37] R. Stassi and F. Nori, Long-lasting quantum memories: Extending the coherence time of superconducting artificial atoms in the ultrastrong-coupling regime, *Phys. Rev. A* **97**, 033823 (2018).
- [38] P. Nataf and C. Ciuti, Protected Quantum Computation with Multiple Resonators in Ultrastrong Coupling Circuit QED, *Phys. Rev. Lett.* **107**, 190402 (2011).
- [39] N. Ofek *et al.*, Extending the lifetime of a quantum bit with error correction in superconducting circuits, *Nature* **536**, 441 (2016).
- [40] P. K. Lam and C. M. Savage, Complete atomic population inversion using correlated sidebands, *Phys. Rev. A* **50**, 3500 (1994).
- [41] G. S. Agarwal, W. Lange, and H. Walther, Intense-field renormalization of cavity-induced spontaneous emission, *Phys. Rev. A* **48**, 4555 (1993).
- [42] M. Macovei, J. Evers, and C. H. Keitel, Spontaneous decay processes in a classical strong low-frequency laser field, *Phys. Rev. A* **102**, 013718 (2020).
- [43] G. S. Agarwal and W. Harshawardhan, Realization of trapping in a two-level system with frequency-modulated fields, *Phys. Rev. A* **50**, R4465 (1994).
- [44] G. S. Agarwal, Spontaneous decay processes in a classical strong low-frequency laser field, *Phys. Rev. A* **61**, 013809 (1999).
- [45] L. O. Castaños, Simple, analytic solutions of the semiclassical Rabi model, *Opt. Commun.* **430**, 176 (2019).
- [46] L. O. Castaños, A simple, analytic solution of the semiclassical rabi model in the red-detuned regime, *Phys. Lett. A* **383**, 1997 (2019).
- [47] G. B. Folland, *Fourier Analysis and its Applications* (American Mathematical Society, Providence, 2009).
- [48] J. Guckenheimer and P. Holmes, *Nonlinear Oscillations, Dynamical Systems, and Bifurcations of Vector Fields* (Springer, New York, 2013).
- [49] C. Cohen-Tannoudji, B. Diu, and F. Laloë, *Quantum Mechanics*, 2nd ed. (Wiley, New York, 2019), Vol. 1.
- [50] L. O. Castaños and A. Zuñiga-Segundo, The forced harmonic oscillator: Coherent states and the RWA, *Am. J. Phys.* **87**, 815 (2019).
- [51] J. Garrison and R. Chiao, *Quantum Optics* (Oxford University, New York, 2008).
- [52] H. P. Breuer and F. Petruccione, *The Theory of Open Quantum Systems* (Oxford University, New York, 2007).
- [53] H. J. Carmichael, *Statistical Methods in Quantum Optics* (Springer, New York, 1999), Vol. 1.
- [54] W. Greiner and J. Reinhardt, *Field Quantization* (Springer-Verlag, Berlin, 1996).